Special Independent Race Models With No Threshold Variability

In preliminary work, we considered two special independent race models that describe the nature of the racing processes in terms of familiar stochastic accumulator models: a diffusion model and a Poisson counter model. Each of the models specifies the finishing time distribution for each runner in the race in terms of two parameters that describe the stochastic accumulation: a rate parameter that describes how quickly information is gained over time and a threshold parameter that describes how much information must be accumulated before a response can be selected. Rate and threshold parameters capture most of the important effects in stochastic accumulator models of RT (Ratcliff & Smith, 2004). We use them to assess the nature of capacity limitations in the stop process and the go process. Neither of the models incorporated threshold variability between trials, like the diffusion race model in the main text.

Diffusion Race Model

The diffusion race model assumes that each stochastic accumulator is a Wiener diffusion process with a drift rate ξ, a starting point at 0, and an absorbing boundary at z (we assume a drift coefficient equal to 1). The accumulator for the stop process does not begin until stop-signal delay expires. Under these assumptions, the finishing time distributions $f_i(t)$ are given by inverse normal (Wald) densities with parameters determined by the drift rate and boundary placement. Thus, for the go process

$$f_i(t) = z\left(2\pi t^3\right)^{-1/2} \exp\left[-\frac{1}{2t}\xi(t + z/\xi)^2\right] \quad (1)$$

and for the stop process

$$f_{stop}(t) = z\left(2\pi (t - t_d)^3\right)^{-1/2} \exp\left[-\frac{1}{2(t - t_d)}\xi(t - t_d + z/\xi)^2\right] \quad (2)$$

if $t > t_d$ and 0 otherwise. We substituted Equations 1 and 2 for the generic distributions in the general independent race model to generate likelihood functions

to fit the diffusion race model to the data. We can use the parameters estimated in fitting Equation 2 to the data to estimate the distribution of SSRTs.

Poisson Counter Race Model

Poisson counter models have been used in a variety of applications, from visual identification (Kyllingsbaek, Markussen & Bundesen, 2012) to attention (Logan, 1996) and recognition memory (Van Zandt, 2000b). Poisson counter models assume that information accumulates in discrete chunks (e.g., neural spikes) until a threshold is reached, and the interval between successive chunks is exponentially distributed with a constant rate (Townsend & Ashby, 1983; Smith & Van Zandt, 2000b; Van Zandt, 2000b; Van Zandt et al., 2000). Under these assumptions, the finishing time distributions for the Poisson counters are gamma with shape parameters equal to the counter thresholds and with rate parameters equal to the exponential interarrival time. Note that the finishing time distribution for the race is not gamma. Instead, it is the distribution of minima from racing gamma distributions. The gamma distribution for each runner approaches the normal distribution as the number of counts (threshold) increases, but the finishing time of the race remains skewed because the other runners in the race filter the upper tail and skew the distribution.

In the Poisson race model, the finishing time distribution for each go response is a gamma distribution, and each can have its own rate and threshold parameter. The finishing time distribution for the stop process is a shifted gamma distribution. The accumulation of counts does not begin until stop-signal delay elapses (i.e., $f_{stop}(t) = 0$ if $t < t_d$ and gamma if $t > t_d$; Smith & Van Zandt, 2000). Thus, for the go processes,

$$f_i(t) = \Gamma(K_i)^{-1}(\lambda_i t)^{K_i - 1}\lambda_i \exp\left[-t\lambda_i\right] \quad (3)$$

if $t > 0$ and 0 otherwise, and for the stop process

$$f_{stop}(t) = \Gamma(K_{stop})^{-1}(\lambda_{stop}(t - t_d))^{K_{stop} - 1}\lambda_{stop} \exp\left[-\lambda_{stop}(t - t_d)\right] \quad (4)$$

if $t > t_d$ and 0 otherwise, where K is the threshold and λ is the exponential rate parameter.[1] We substituted Equations 3 and 4 for the generic distributions in the general independent race model to generate likelihood functions to fit the Poisson race model to the data. We can use the parameters estimated in fitting Equation 4 to the data to estimate the distribution of SSRTs.

Experiment 1: Stopping Multiple-Choice RT

To evaluate the special race models and test the hypothesis that stop and go processes share capacity, we conducted an experiment in which six subjects each performed a multiple-choice RT task combined with a stop-signal task for 12 sessions. The method and results are reported in the main text. To evaluate the nature of capacity limitations in the stop and go processes, we fit eight versions of the diffusion race model and eight versions of the Poisson race model to the multiple-choice data for correct and error responses. For the diffusion race models, we used Equations 1 and 2 to generate likelihood functions; for the Poisson race models, we used Equations 3 and 4. For each model, we assumed there was one runner in the race for each choice alternative in the go task and one runner for the stop task. The go runners were characterized by a rate and a threshold parameter. Within a set of choice alternatives, the correct response had a rate parameter of ξ_i (diffusion race) or λ_i (Poisson race) and each incorrect response had a rate parameter of ε_i (diffusion race) or μ_i (Poisson race). The rates were the same for each incorrect response in the set. There was one threshold z_i (diffusion race) or K_i (Poisson race) for all responses in a set of choice alternatives, though in different models the threshold could vary between sets of choice alternatives. The stop process had one rate parameter, ξ_{stop} (diffusion race) or λ_{stop} (Poisson race), and one threshold, z_{stop} (diffusion race) or K_{stop} (Poisson race). There were two separate non-decision time parameters, one for the stop process and one for the go process, but

[1] We allowed K to take on continuous values, as opposed to strictly integer values, for ease of model fitting. This does not change the psychological interpretation of K as a threshold. and λ as the exponential rate parameter.

within each process, non-decision time was not allowed to vary with number of choice alternatives (cf. Leite & Ratcliff, 2010).

The eight versions of the diffusion and Poisson race models differed in their assumptions about whether rates and thresholds for the go and stop processes were held constant or were allowed to vary with the number of choice alternatives. We tested hypotheses about capacity limitations in the go process by comparing models in which go rates were constant (unlimited capacity) or varied (limited capacity) with the number of choice alternatives. We tested hypotheses about shared capacity limitations in stop and go processes by comparing models in which stop rates were constant (unshared capacity) or varied (shared capacity) with the number of choice alternatives. The models and their assumptions are presented in Table S1. Each model is characterized by four letters indicating whether go thresholds, go rates, stop thresholds, and stop rates (respectively) were held constant (C) or allowed to vary (V) with the number of choice alternatives.

Diffusion race model fits. Of the eight models, the one that fit best assumed a limited-capacity go process and an unlimited-capacity stop process (model VVCC in Table S1). This model produced the lowest BIC score aggregated across subjects and the lowest BIC score in four out of six subjects (see Table S2). The predicted mean go RTs, mean SSRTs and error rates (points) are plotted with the observed values (lines) in Figure S1. The model predicts no-stop-signal RT and signal-respond RT well but it over-predicts error rate. The predicted inhibition functions (points) are plotted with the observed inhibition functions (lines) in Figure S2, showing close agreement. The predicted RT distributions (points) are plotted with the observed values (lines) in Figure S3. Like the observed values, the predicted values fanned out from a common minimum, with longer upper tails for longer stop-signal delays.

The values of the best-fitting parameters for model VVCC, averaged across subjects, are presented in Table S3. The rate parameters for the go process decreased as number of choice alternatives increased, indicating limited capacity. The sum of the rates decreased from two choices ($\xi_{2go} + \varepsilon_{2go} = 0.229$) to four choices

($\xi_{4go} + 3\varepsilon_{4go} = 0.216$) to six choices ($\xi_{6go} + 5\varepsilon_{6go} = 0.157$), indicating stronger capacity limitations than a fixed-capacity model would predict. The rate parameters for the stop process were constrained to be the same for each number of choice alternatives, suggesting that the stop process and the go process do not share capacity.

The fits to the individual subject data were mostly consistent with the aggregate fits. The limited-capacity go, unshared-capacity stop model (VVCC) fit best for Subjects 1, 3, 4, and 6. The limited-capacity go, shared-capacity stop model (VVCV) fit best for Subject 2, whose "observed" SSRTs increased with number of choice alternatives, indicating a limited-capacity stop process. The unlimited-capacity go, unshared-capacity stop model (VCCC) fit best for Subject 5. On the one hand, the fit for Subject 5 is consistent with the majority of subjects in suggesting an unlimited capacity stop process. On the other hand, the fit for Subject 5 suggests an unlimited capacity go process, which would not share capacity with the stop process, so this fit does not address the question of whether the stop and go process share capacity as directly as the other fits that show a limited-capacity go process.

Poisson race model fits. The Poisson race model fits were largely consistent with the diffusion model fits. The limited-capacity go, unshared-capacity stop model (VVCC) fit best in the aggregate BIC scores and in three of the six individual subjects (Subjects 2, 5, and 6; see Table S2). Limited-capacity go, shared-capacity stop (VVCV) fit best for Subject 1, whose "observed" SSRTs increased with number of choices, and for Subject 3, whose "observed" SSRTs did not increase with the number of choices. The predictions of the limited-capacity go, unshared-capacity stop model (VVCC) are plotted along with the observed values in Figures S1, S2, and S3, showing good agreement between predicted and observed values.

The values of the best-fitting parameters are presented in Table S3. The rates for the go process decreased with the number of choice alternatives, consistent with limited capacity. The sum of the rates was about the same for each number of choice alternatives ($\lambda_{2go} + \mu_{2go} = 0.033$; $\lambda_{4go} + 3\mu_{4go} = 0.034$; $\lambda_{6go} + 5\mu_{6go} = 0.029$), suggesting fixed capacity. The rates for the stop process were constrained to

be the same for each number of choice alternatives, suggesting that the limited- or fixed-capacity go process did not share capacity with the stop process.

SSRT distributions. SSRT distributions for the best-fitting aggregate model (VVCC) are plotted in Figure S5.

Correct and error RT distributions. Predicted and observed distributions of correct and error RTs are plotted in Figure S6. The diffusion race model and the Poisson race model predicted RT distributions for correct responses well but they both over-predicted error RTs. We tried to remedy this over-prediction by incorporating threshold variability in the diffusion race model presented in the main text.

Linear Ballistic Accumulator Model

We the Linear Ballistic Accumulator (LBA) model (Brown & Heathcote, 2008) to determine whether it could account for error RT distributions in the multiple-choice data. LBA has accounted for error RT distributions accurately in past applications, so it seemed promising here. We implemented one version of LBA that assumed variable thresholds and variable rates in the go process but fixed thresholds and fixed rates in the stop process (i.e., model VVCC) because diffusion and Poisson race models with those assumptions provided the best fit to the data.

LBA fit the data about as well as the diffusion race and Poisson race models. The likelihoods, AIC, and BIC scores for individual subjects and the aggregate BIC score are presented in Table S4. The fit was about as good as the fit of the diffusion race model reported in the article: the aggregate BIC was 590974 for LBA and 590736 for the diffusion race model. The predicted RT distributions for correct and error no-stop-signal trials are presented in Figure S7. LBA predicted the correct RT distributions accurately, but it over-predicted the error RT distributions. Because LBA accounted for error RT distributions well in past applications (Brown & Heathcote, 2008), we attribute its failure in the present case to the small amount of error data (around 2%) rather than to the inability of the model to account for error RTs.

Experiment 2: Stopping Short-Term Memory Search

To evaluate the special race models and test the hypothesis that stop and go processes share capacity, we conducted an experiment in which six subjects each performed a short-term memory search task (Sternberg, 1969, 1975) combined with a stop-signal task for 24 sessions. The short-term memory search task has been modeled with (Atkinson, Holmgren & Juola, 1969) and without (Nosofsky, Little, Donkin, & Fific, 2011) assuming capacity limitations. Under many conditions, limited- and unlimited-capacity models of the memory search task mimic each other (Townsend & Ashby, 1983).

The memory search task required subjects to decide whether a probe word was a member of a set of one, two, or three 5-letter words that was presented at the beginning of each trial, by pressing one key for a "yes" response and another key for a "no" response. The stop signal was a tone that was presented on 25% of the trials at stop-signal delays that were set separately for each subject and each choice condition to correspond to the 15^{th}, 35^{th}, 55^{th}, 75^{th}, and 95^{th} percentile of the subject's go RT distribution for that condition. The stop-signal delays were based on a practice block with no stop signals in the first session and remained the same throughout all 24 sessions. New words were used in each session to keep go RT relatively constant (Logan, 1978). There were 240 trials in each memory set size each session, yielding a total of 17,280 trials per subject for model fitting.

Method

Subjects. Six people from the Vanderbilt University community participated for monetary compensation ($12/hour). All subjects had normal or corrected-to-normal vision and all were naive as to the purpose of the experiment.

Apparatus and stimuli. The experiment was run on a Pentium 4 PC. The stimuli were presented on a 21-inch cathode ray tube monitor. In the go task, subjects had to decide whether a target word was presented in a study phase. Half of the subjects pressed '*Z*' when the target word was in the study list (*target-present* trials), and '/' when it was not (*target-absent* trials); this mapping was reversed for the other half of the subjects. The words were presented centrally in a white

uppercase Courier font (size = 16) on a black background. We used the same pool of words we used in Experiment 1, selecting a separate sample of 12 different words for each session. The stop signal was a loud and clear auditory tone (80dB, 100 ms, 500Hz) presented through closed headphones (Sennheiser eH150).

Procedure. The experiment consisted of 24 sessions. At the beginning of the first session, instructions were given orally by the experimenter. Subjects were instructed to respond as quickly and accurately as possible. In each session, there were three conditions varying in memory set size (1, 2 or 3). Each trial consisted of a study phase and a test phase. One, two or three words were selected randomly from the set of 12 for each study phase. Set size varied randomly within each block. The test word matched one of the words in the study phase on half of the trials (*target present* trials) and did not match any of the words in the study phase on the other half of the trials (*target absent* trials). Target-present and target-absent trials varied randomly throughout each block.

Each trial started with a blank screen. After 400 ms, one, two or three words were presented (the *study phase*). For set size 1, the study word occurred at one of three locations at random: 25 pixels above the center of the screen, the center of the screen, or 25 pixels below the center of the screen. A filler string (++++++) occurred in the two 'non-occupied' locations. For set size 2, two study words were presented and the filler string appeared in the top, middle, or bottom position. For set size 3, each position contained a study word. The duration of the study phase was 800 ms for set size 1, 1,600 ms for set size 2, and 2,400 ms for set size 3. After the study phase, all words were replaced by filler strings. After 400 ms, the target word was presented in the center of the screen and remained on the screen for 1,000 ms, regardless of RT. Subjects had to decide whether the target was present in the study phase. On target-present trials, the target matched one of the words from the study phase, selected at random. On target-absent trials, the target was not presented in the study phase but selected randomly from the remaining words in the 12-word list.

Stop signals were presented on 25% of the trials at a variable delay that was based on performance in the stop-signal practice block in Session 1. For each set

size, stop-signal delay was 15%, 35%, 55%, 75%, or 95% of the corresponding mean RT in the practice phase. We used different SSDs for target-present and target-absent trials. Thus, for target-absent set size 3, we used the mean RT of the target-absent trials for set size 3. Delays were randomized and occurred with equal probability.

The experiment consisted of 24 sessions. The first session started with a practice block of 30 trials without stop signals. This no-stop-signal block was followed by another practice block of 120 trials with stop signals. All other sessions started with a practice block of 30 trials without signals and a practice block of 60 trials with stop signals. After the practice phase, there were six experimental blocks of 120 trials in all sessions. At the end of each block, we presented the number of no-stop-signal errors, the mean RT and the probability of stopping. Subjects had to pause for 10 seconds.

Results: Behavioral Data

Mean RTs for correct responses, collapsed across subjects and sessions, are plotted as a function of memory set size and target presence (yes) and absence (no) in Figure S8. Mean no-stop-signal RT increased with memory set size, as usual (Sternberg, 1975). The increase was approximately linear and the slope was the same for "yes" responses (32 ms/item) as for "no" responses (32 ms/item). The slopes were stable across sessions because we changed memory sets every session (Logan, 1978). Summary tables for 2 (target present vs. absent) x 3 (set size) analyses of variance on mean no-stop-signal RTs, signal-respond RTs, SSRTs, and error rates appear in Table S5.

Consistent with the stop-signal literature, mean signal-respond RTs were faster than no-stop-signal RTs, as usual (Logan & Cowan, 1984). They also increased approximately linearly with set size. The slope was 32 ms/item for "yes" responses and 22 ms/item for "no" responses. Inhibition functions across subjects and sessions are plotted as a function of stop-signal delay for "yes" and "no" responses at each memory set size in Figure S8. Consistent with the stop-signal

literature, the probability of responding given a stop signal increased with stop-signal delay.

We calculated mean SSRT for each subject using the integration method (Logan & Cowan, 1984). The means across subjects and sessions for "yes" and "no" responses are plotted in Figure S8 as a function of memory set size. There was no tendency for mean SSRT to increase with memory set size. For "yes" responses, mean SSRT decreased by 7 ms from set size 1 to 3; for "no" responses, it decreased by 6 ms from set size 1 to 3. These small negative differences contrast with the larger positive differences found for no-stop-signal RTs (M = 64 ms) and signal-respond RTs (M = 27 ms) in the go task, suggesting that the stop process does not share capacity with the go process. The modeling results will allow us to assess this hypothesis more rigorously.

Results: Special Race Model Fits

To evaluate capacity limitations in the stop and go processes, we fit eight diffusion race models and eight Poisson race models to the memory-search data (see Table S1). For the go process, each model assumed a race between two runners, one for "yes" responses and one for "no" responses. The rate parameter was ξ_i (diffusion race) or λ_i (Poisson race) if the probe matched the memory item (i = yes) or a lure (i = no) and ε_i (diffusion race) or μ_i (Poisson race) if it did not. The threshold was z_i (diffusion race) or K_i (Poisson race). Rates and thresholds were allowed to differ for "yes" and "no" responses. For the stop process, each model assumed a single runner with rate ξ_i (diffusion race) or λ_i (Poisson race) and threshold z_i (diffusion race) or K_i (Poisson race). The eight models differed in their assumptions about variation in the rate and threshold parameters across memory set size (see Table S1). For the go process, variable rates reflect limited capacity and constant rates reflect unlimited capacity. For the stop process, variable rates reflect shared capacity and constant rates reflect unshared capacity.

Diffusion race model fits. The BIC scores for all subjects and models appear in Table S6. As with the multiple-choice data, the model that fit the memory search

data best assumed a limited-capacity go process and an unlimited-capacity stop process (model VVCC). Model VVCC produced the lowest aggregate BIC and the lowest individual-subject BIC for three of the six subjects (Subjects 1, 5, and 6). The best-fitting models for the other subjects (VVVC for Subjects 2 and 3; CVCC for Subject 4) also assumed an unlimited-capacity stop process.

The predicted values for the best-fitting model (VVCC) appear in Figures S8, S9, and S10. The VVCC model predicted go RTs accurately, for both no-stop-signal and signal-respond trials (Figure S8). It predicted target-present error rate well but under-predicted target-absent error rate (Figure S8). It over-predicted the SSRTs estimated by the integration method. The VVCC model predicted inhibition functions (Figure S9) and RT distributions (Figure S10) well, capturing the effect of stop-signal delay in both data sets.

The values of the best-fitting parameters for model VVCC, averaged across subjects, are presented in Table S7. The rate parameters for the go process decreased as memory set size increased, indicating limited capacity. The sum of the rate parameters ($\xi_{iyes} + \varepsilon_{iyes} + \xi_{ino} + \varepsilon_{ino}$) decreased as memory set size increased (0.695, 0.602 and 0.671 for set sizes 1-3, respectively), suggesting that capacity limitations were stronger than a fixed-capacity model would predict (Logan, 1978). The rate parameters for the stop process were held constant across memory set size, implementing unshared capacity.

Poisson race model fits. The BIC scores for each model and subject are presented in Table S6. The best-fitting Poisson race model assumed a limited-capacity go process and an unshared-capacity stop process (model VVCC). It produced the lowest aggregate BIC and the lowest individual-subject BICs in Subjects 3, 4, and 5 (see Table S3). The predicted values for the best-fitting model (VVCC) appear in Figures S8 (mean go RT, signal-respond RT, SSRT and error rate), Figure S9 (inhibition functions), and Figure S11 (no-stop-signal and signal-respond RT distributions). The figures show good agreement between observed and predicted values, except for under-predicting the increase in target-absent error rate with memory set size.

The best-fitting parameters for the limited-capacity go, unlimited-capacity stop model (VVCC) are presented in Table S7. The rate parameters for the go process varied with memory set size but did not decrease monotonically. The sums of the rate parameters ($\lambda_{iyes} + \mu_{iyes} + \lambda_{ino} + \mu_{ino}$) did not change as memory set size increased (0.109, 0.091, and 0.109 for set sizes 1-3, respectively), suggestive of fixed capacity. The rate parameters for the stop process were held constant to implement unshared capacity.

SSRT distributions. The predicted parent and winning distributions of SSRT for the best-fitting diffusion and race Poisson models (VVCC) are plotted in Figure S12.

Correct and error RT distributions. Predicted and observed distributions of correct and error RTs are plotted in Figure S13. The diffusion race model and the Poisson race model predicted RT distributions for correct responses well but they both over-predicted error RTs.

Strategic Slowing and Stop-Signal Probability

Bissett and Logan (2011, Experiment 1) conducted an experiment in which 24 subjects performed a stop-signal task in which stop signals occurred on 20% or 40% of the trials. The go task involved classifying shapes into one of two categories. The stop signal was a tone. Stop-signal delay was adjusted with a tracking procedure that produced successful stopping on 50% of stop-signal trials. Stop-signal probability was manipulated within subjects between sessions. There were 1,200 trials in each session for a total of 2,400 trials per subject.

The manipulation of stop signal probability pits the go task directly against the stop task. A reduction in the probability of the go task is accompanied by an increase in the probability of the stop task. This invites a tradeoff between stopping and going that would be expected if the stop process and go process shared capacity or utility. We will look for evidence of a tradeoff by examining the parameters of the best fitting diffusion race models. A tradeoff would be evident as an opposite shift in parameter values for the stop and go diffusions between the 20% and 40%

conditions. If go and stop processes trade capacity, the go rate might increase while the stop rate decreases. If the go and stop processes trade utility, the go threshold might increase as the stop threshold decreases.

Results. The mean go RTs, signal-respond RTs, SSRTs, and error rates across subjects are plotted against percentage of stop signals in Figure S1. Subjects responded appropriately to the stop signal, inhibiting their responses on 50% of the trials in both conditions. They responded to the go task more slowly when stop signals were more frequent. Mean go RT was 514 ms with 40% stop signals and 459 ms with 20% stop signals. Accuracy was equivalent in the two conditions (93%). SSRT was faster with 40% stop signals (M = 224 ms) than with 20% stop signals (M = 243 ms), but the difference was not significant.

Diffusion race model fits. We fit a set of 16 diffusion race models to the data from Bissett and Logan (2011). The set was created from the factorial combination of fixing versus varying go rate, go threshold, go non-decision time, and stop-process parameters between the 20% and 40% stop signal conditions. The models are described in Table S8. All stop process parameters (rate, threshold, non-decision time) were fixed together or varied together in a particular model.

Each of the 16 models assumed two go runners and one stop runner. The drift rates were ξ_i for the correct go response and ε_I for the incorrect go response. The threshold was z_i for both go responses. The stop process drift rate was ξ_{stop} and its threshold was z_{stop}. Both thresholds varied uniformly between $z_i - a_i$ and $z_i + a_i$ to capture error RT distributions. The stop and go processes had separate non-decision times. The models differed in which of these parameters were fixed and varied between the 20% and the 40% conditions. We generated a likelihood function for each model and fit it to the data by minimizing BIC. We compared model fits with aggregate BICs and with BICs for individual subjects.

The BIC values from the aggregate fits are presented in Table S7. In the aggregate fits, the best fitting model was one that let go rate vary between conditions, and held everything else constant, suggesting no tradeoff between stop and go processes (row 9 in Table S7). The predictions from this model, averaged

over subjects, are plotted with the observed data in Figure S14. The model captured the trends in the means, but the predictions were not perfect. The model under-predicted signal-respond RT in the 20% condition, and it under-predicted SSRT in both conditions. It over-predicted error rate in the 40% condition, although it did predict the observed decrease in error rate from the 20% to the 40% condition.

The no-signal and signal-respond RT distributions predicted by the model that fit the aggregate best (go rate changes; go threshold, stop threshold, stop rate fixed) are plotted with the observed values in Figure S15. The model predicted the no-signal and signal-respond distributions accurately with 40% stop signals, and it predicted the no-signal distribution accurately with 20% stop signals. However, the model under-predicted the signal-respond distribution with 20% stop signals. We suggest two interpretations of this under-prediction. First, it may reflect a problem with the model. The model may not be able to predict signal-respond distributions accurately. We think this is unlikely. The model predicted signal-respond distributions accurately in all of the fits so far, including the one in the 40% stop signal condition. Moreover, the predictions seem right. The proportional reduction in signal-respond RT is about the same in the two conditions: The predicted mean signal-respond RT is 11% faster than the predicted mean no-signal RT in the 20% stop signal condition. It is 12% faster in the 40% condition. Second, the under-prediction may result from a problem with the data. Some subjects in the 20% condition may have violated the context independence assumption of the race model (Equation 6), producing longer signal-respond RTs than would be expected if stopping and going were independent. Indeed, the predicted signal-respond distribution is exactly what would be predicted assuming context and stochastic independence. This is an important question for future research.

The individual fits did not show much consensus on the best-fitting model. Ten of the 16 models fit best for at least one subject: Three models fit best for four subjects each, one model fit best for three subjects, three models fit best for two subjects each, and three models were fit best for one subject each. Fifteen of the 24 subjects were fit better by models with go rates varied than with go rates fixed, while 20 of the 24 subjects were fit better by models with stop rates fixed than with

stop rates varied. Thus, there is no evidence of a tradeoff at the individual subject level. Thirteen subjects were fit better by models with go thresholds fixed, while 20 subjects were fit better by models with stop thresholds fixed.

The best-fitting parameter values are plotted against stop signal percentage in Figure S16. The top panel contains the average parameters for the model that fit the aggregate data best. Go rate decreased as percentage of stop signals increased, but the other parameters remained constant. Thus, there was no tradeoff between stopping and going in this model. The bottom panel contains the average of the parameter values over the models that fit each individual subject best. There was a suggestion of a tradeoff in drift rate: Go rate decreased and stop rate increased from 20% to 40% stop signals. However, there was no evidence of a tradeoff in threshold. Thresholds for both stop and go processes increased from 20% to 40% stop signals.

The distributions of predicted SSRTs for the 20% and 40% stop signals condition are presented in Figure S17.

The distributions of correct and error RTs are plotted in the top panel of Figure S18. The points are observed values and the lines are predictions from the model that fit the aggregate best (varied go rate, fixed stop rate, go threshold, and stop threshold). Defective distributions of correct and error RTs are plotted in the bottom panel, following the same convention. The model predicted correct RTs accurately, and it over-predicted error RTs. This time, however, the over-prediction was not as large as it was in previous fits. The mean difference between predicted and observed error RTs was 46 ms in the 20% condition and 51 ms in the 40% condition. By contrast, in the Verbruggen and Logan (2009c) fits, the mean difference between predicted and error RTs was 90 ms in the “none” condition and 89 ms in the “all” condition. In the fits to the 2-choice multiple choice data, the mean difference was 83 ms. We view this as an improvement in the fit, and we suggest it resulted from a higher error rate in this experiment (9% in the 20% condition; 8% in the 40% condition) than in the previous ones (2% in the multiple-choice experiment; 3% in Verbruggen & Logan, 2009c).

Discussion. The model fits suggest that the slowing with higher stop signal percentages observed by Bissett and Logan (2011, Experiment 1) was primarily due to a reduction in the go task drift rate. The go task threshold, and the stop drift rate and threshold did not change much. They were constant in the aggregate fits and changed by a small amount in the average of individual subject fits. There was little evidence of a tradeoff between stop and go tasks in the best-fitting parameters.

We were surprised to find that slowing was due to drift rate rather than threshold. We thought the slowing was strategic, and so would be produced by increasing the threshold, as in the fits to Verbruggen and Logan (2009c). However, the data show no evidence of a speed-accuracy tradeoff that would require a model to increase threshold. RT increased but error rate was unchanged as stop signal percentage increased (Bissett & Logan, 2011). This is inconsistent with several studies that manipulated stop signal percentage and found a reduction in error rate (Logan, 1981; Ramautar et al., 2004; Verbruggen & Logan, 2009c), but consistent with at least one previous study (Logan & Burkell, 1986). Thus, subjects may respond to stop signal percentage manipulations in different ways. This is reinforced by the diversity of best-fitting models in our fits to individual subjects: 10 of the 16 models fit at least one subject best.

The reduction in go-task drift rate could be interpreted as an intentional, top-down effect if there was evidence of a tradeoff between going and stopping. A tradeoff would predict a corresponding increase in stop-task drift rate. There was no such tradeoff in the aggregate fits, but a weak tradeoff in the averages of the best-fitting parameters across subjects. This possible tradeoff suggests the stop and go tasks share capacity, but that is ruled out by the multiple-choice results (also see Yamaguchi et al., 2012). Instead, stop and go tasks may share utility or value.

The reduction in go-task drift rate could also be interpreted as an unintentional top-down effect. The go task depends on active maintenance of a task set for responding, and that task set may decay when subjects are busy with the stop task (Altmann & Gray, 2008). The more stop signals, the greater the opportunity for decay. This effect can be understood in Logan and Gordon's (2001) ECTVA model, in which a task set is a set of parameters controlled by the executive, and drift rate is

the product of a top-down bias parameter that the executive controls and a bottom-up similarity parameter that reflects the match between the stimulus and a memory representation (also see Bundesen, 1990; Logan, 2002; Nosofsky & Palmeri, 1997). ECTVA assumes bias parameters are set in working memory, so they may decay if working memory is occupied with dealing with a stop trial (Logan, 1979). Smaller bias parameters would reduce drift rates, and produce longer RTs. Future research may distinguish these interpretations.

References

Altmann, E. M., & Gray, W. D. (2008). An integrated model of cognitive control in task switching. *Psychological Review, 115,* 602-639.

Ashby, F. G., & Townsend, J. T. (1986). Varieties of perceptual independence. *Psychological Review, 93,* 154-179.

Atkinson, R. C., Holmgren, J. E., & Juola, J. F. (1969). Processing time as influenced by the number of elements in a visual display. *Perception & Psychophysics, 6,* 321-326.

Bissett, P. G., & Logan, G. D. (2011). Balancing cognitive demands: Control adjustments in the stop-signal paradigm. *Journal of Experimental Psychology: Learning, Memory and Cognition, 37,* 392-404.

Cavanagh, J. P. (1972). Relation between the immediate memory span and the memory search rate. *Psychological Review, 79,* 525-530.

Garner, W. R. (1962). *Uncertainty and structure as psychological concepts.* Oxford: Wiley.

Hick, W. E. (1952). On the rate of gain of information. *Quarterly Journal of Experimental Psychology, 4,* 11-26.

Hyman, R. (1953). Stimulus information as a determinant of reaction time. *Journal of Experimental Psychology, 45,* 188-196.

Kyllingsbaek, S., Markussen, B. & Bundesen, C. (2012). Testing a Poisson counter model for visual identification of briefly presented, mutually confusable single stimuli in pure accuracy tasks. *Journal of Experimental Psychology: Human Perception and Performance, 38*, 628-642.

Leite, F. P., & Ratcliff, R. (2010). Modeling reaction time and accuracy of multiple-alternative decisions. *Attention, Perception & Psychophysics, 72,* 246-273.

Logan, G. D. (1978). Attention in character classification: Evidence for the automaticity of component stages. *Journal of Experimental Psychology: General, 107,* 32-63.

Logan, G. D. (1979). On the use of a concurrent memory load to measure attention and automaticity. *Journal of Experimental Psychology: Human Perception and Performance, 5,* 189-207.

Logan, G. D. (1988). Toward an instance theory of automatization. *Psychological Review, 95,* 492-527.

Logan, G. D. (1996). The CODE theory of visual attention: An integration of space-based and object-based attention. *Psychological Review, 103,* 603-649.

Logan, G. D. & Burkell, J. (1986). Dependence and independence in responding to double stimulation: A comparison of stop, change, and dual-task paradigms. *Journal of Experimental Psychology: Human Perception and Performance, 12,* 549-563.

Logan, G. D. & Cowan, W. B. (1984). On the ability to inhibit thought and action: A theory of an act of control. *Psychological Review, 91,* 295-327.

Myung, I. J. (2003). Tutorial on maximum likelihood estimation. *Journal of Mathematical Psychology, 47,* 90-100.

Nosofsky, R. M., Little, D. R., Donkin, C., & Fific, M. (2011). Short-term memory scanning viewed as exemplar-based categorization. *Psychological Review, 118,* 280-315.

Nosofsky, R. M., & Palmeri, T. J. (1997). An exemplar-based random walk model of speeded classification. *Psychological Review, 104,* 266-300.

Ramautar, J. R., Kok, A., & Ridderinkhof, K. R. (2004). Effects of stop signal probability in the stop-signal paradigm: The N2/P3 complex further validated. *Brain and Cognition, 56,* 234-252.

Ratcliff, R. (1978). A theory of memory retrieval. *Psychological Review, 85,* 59-108.

Ratcliff, R., & Smith, P. L. (2004). A comparison of sequential sampling models for two-choice reaction time. *Psychological Review, 111,* 333-367.

Ratcliff, R., Van Zandt, T., & McKoon, G. (1999). Connectionist and diffusion models of reaction time. *Psychological Review, 106*, 261-300.

Rieger, M., & Gauggel, S. (1999). Inhibitory after-effects in the stop signal paradigm. *British Journal of Psychology, 90,* 509-518.

Smith, P. L., & Van Zandt, T. (2000). Time dependent Poisson counter models of response latency in simple judgment. *British Journal of Mathematical and Statistical Psychology, 53,* 293-315.

Sternberg, S. (1966). High-speed scanning in human memory. *Science, 153,* 652-654.

Sternberg, S. (1975). Memory scanning: New findings and current controversies. *Quarterly Journal of Experimental Psychology, 27,* 1-32.

Townsend, J. T., & Ashby, F. G. (1983). *Stochastic modeling of elementary psychological processes.* Cambridge: Cambridge University Press.

Table S1

Models fitted to the multiple choice data in Experiment 1 and the memory search data in Experiment 2. The best-fitting model over subjects in both experiments is in bold font.

Name	Go Threshold	Go Rate	Stop Threshold	Stop Rate	Go Capacity	Stop Capacity	Param Expt 1	Param Expt 2
VVVV	Varied	Varied	Varied	Varied	Limited	Limited	17	24
VVCC	**Varied**	**Varied**	**Constant**	**Constant**	**Limited**	**Unlimited**	**13**	**20**
VVVC	Varied	Varied	Varied	Constant	Limited	Unlimited	15	22
VVCV	Varied	Varied	Constant	Varied	Limited	Limited	15	22
VCVV	Varied	Constant	Varied	Varied	Unlimited	Limited	13	14
CVVV	Constant	Varied	Varied	Varied	Limited	Limited	15	19
VCCC	Varied	Constant	Constant	Constant	Unlimited	Unlimited	9	10
CVCC	Constant	Varied	Constant	Constant	Limited	Unlimited	11	15

Note: Varied = parameter is allowed to vary with number of choice alternatives; Constant = parameter is held constant across number of choice alternatives; Param = Number of Parameters.

Table S2

Bayesian Information Criterion (BIC) scores for models fit to the multiple choice data from Experiment 1 for each subject and aggregated over subjects. The BIC score for the best model is in bold font.

Diffusion Model	Subject 1	Subject 2	Subject 3	Subject 4	Subject 5	Subject 6	Aggregate BIC
VVVV	103830	98166	95980	92606	98114	102043	590740
VVCC	**103823**	98200	**95960**	92596	**98082**	**101949**	**590610**
VVVC	103849	98149	95967	92624	98097	101992	590678
VVCV	103847	**98132**	95982	92606	98102	101991	590661
VCVV	104942	99249	96066	96066	98264	103256	597844
CVVV	103860	98214	96119	92887	98218	102105	591402
VCCC	104936	99334	96039	**92556**	98221	103212	594297
CVCC	103854	98262	96099	92863	98189	102092	591360
Poisson Model	Subject 1	Subject 2	Subject 3	Subject 4	Subject 5	Subject 6	Aggregate BIC
VVVV	103797	98237	96241	92995	98287	101783	591339
VVCC	103802	**98199**	96260	93013	**98255**	**101759**	**591286**
VVVC	103816	98235	96237	92997	98270	101771	591325
VVCV	**103783**	98240	**96211**	92997	98298	101765	591294
VCVV	104785	104785	96345	93007	98403	102925	600250
CVVV	103873	103873	96297	93145	98325	101858	597371
VCCC	104779	99051	96335	**92957**	98641	102895	594658
CVCC	103864	98300	96366	93110	98286	101833	591759

Table S3

Mean parameter values across subjects for the best fitting diffusion and Poisson models in Experiment 1, which assumed a limited-capacity go process and an unlimited-capacity stop process (Model VVCC in Table S1).

Diffusion	Go			Stop		
N Choices	2	4	6	2	4	6
Threshold (z)	61.89	69.77	68.31	6.43	6.43	6.43
Correct Rate (ξ)	0.192	0.156	0.132	0.099	0.099	0.099
Incorrect Rate (ε)	0.037	0.020	0.005			
Non-Decision Time	160	160	160	229	229	229

Poisson	Go			Stop		
N Choices	2	4	6	2	4	6
Threshold (K)	5.69	6.32	5.63	1.51	1.51	1.51
Correct Rate (λ)	0.027	0.019	0.014	0.020	0.020	0.020
Incorrect Rate (μ)	0.006	0.005	0.003			
Non-Decision Time	259	259	259	198	198	198

Table S4

Likelihood, AIC and BIC scores for fits of a Linear Ballistic Accumulator model that assumed variable go thresholds, variable go rates, fixed stop thresholds, and fixed stop rates (model VVCC) to the multiple-choice data in Experiment 1.

Data	N Observed	N Parameters	Likelihood	AIC	BIC
Subject 1	8635	21	51105.89	102253.79	102402.12
Subject 2	8632	21	49527.25	99096.50	99244.82
Subject 3	8626	21	48035.21	96112.41	96260.73
Subject 4	8639	21	45886.65	91815.31	91963.65
Subject 5	8640	21	48765.43	97572.86	97721.21
Subject 6	8622	21	51482.88	103007.76	103156.06
Aggregate	51794	21	294803.31	589858.62	590974.36

Table S5

Summary tables for 2 (target present vs. absent) x 3 (memory set size: 1, 2, 3) analyses of variance on no-stop-signal response times (RTs), signal-respond RTs, stop signal RTs (SSRTs), and error rates in Experiment 2.

Dependent Variable	Effect	*F* ratio	Degrees of Freedom	Mean Squared Error	*p*
No-Stop-Signal RT					
	Set Size (S)	21.7	2, 10	586	< .001
	Target Presence (T)	0.1	1, 5	4058	> .73
	S x T	1.7	2, 10	410	> .23
Signal-Respond RT					
	Set Size (S)	22.4	2, 10	549	< .001
	Target Presence (T)	0.4	1, 5	3780	> .54
	S x T	1.4	2, 10	517	> .29
SSRT					
	Set Size (S)	0.6	2, 10	67	> .58
	Target Presence (T)	1.8	1, 5	192	> .23
	S x T	0.0	2, 10	149	> .97
Error Rate					
	Set Size (S)	28.3	2, 10	0.00016	< .001
	Target Presence (T)	16.8	1, 5	0.00088	< .01
	S x T	23.3	2, 10	0.00008	< .001

Table S6

Bayesian Information Criterion (BIC) scores for models fit to the memory search data from Experiment 2 for each subject and aggregated over subjects. The BIC score for the best model is in bold font.

Diffusion Model	Subject 1	Subject 2	Subject 3	Subject 4	Subject 5	Subject 6	Aggregate BIC
VVVV	194238	187236	193748	203839	194069	193810	1167199
VVCC	**194200**	187234	193760	203897	**194040**	**193772**	**1167118**
VVVC	194295	**187159**	**193745**	203934	194091	193786	1167246
VVCV	194201	194201	193762	203932	194061	193786	1167150
VCVV	196451	187721	193892	203959	194380	194169	1170723
CVVV	196375	187477	193824	203519	194040	194015	1169454
VCCC	196428	187544	193848	203934	194269	194153	1170178
CVCC	196351	187461	193776	**203480**	194043	193916	1169189
Poisson Model	Subject 1	Subject 2	Subject 3	Subject 4	Subject 5	Subject 6	Aggregate BIC
VVVV	194836	187943	194154	203528	194169	194636	1169523
VVCC	194771	187883	**194076**	**203487**	**194123**	194802	**1169357**
VVVC	194759	187442	194096	203507	195080	**194625**	1169746
VVCV	**194699**	**187178**	194103	203504	194994	194662	1169376
VCVV	196732	188365	194245	204278	195308	195362	1174439
CVVV	195994	187769	194182	203729	194216	194657	1170750
VCCC	196788	188296	194203	204241	195291	194882	1173700
CVCC	195967	187670	194148	203696	194153	194628	1170423

Table S7

Mean parameter values across subjects for best-fitting diffusion and Poisson models in Experiment 2, which assumed a limited-capacity go process and an unlimited-capacity stop process (Model VVCC in Table 1).

Diffusion	Go	Yes		Go	No		Stop		
Set Size	1	2	3	1	2	3	1	2	3
Threshold (z)	114.3	117.6	121.4	101.0	102.5	108.6	17.1	17.1	17.1
Correct Rate (ξ)	0.239	0.227	0.222	0.213	0.203	0.198	0.137	0.137	0.137
Incorrect Rate (ε)	0.143	0.086	0.154	0.100	0.086	0.104			
Non-Decision Time	24	24	24	24	24	24	203	203	203

Poisson	Go	Yes		Go	No		Stop		
Set Size	1	2	3	1	2	3	1	2	3
Threshold (K)	14.17	13.72	16.68	12.27	11.99	13.06	2.05	2.05	2.05
Correct Rate (λ)	0.038	0.033	0.038	0.035	0.032	0.031	0.021	0.021	0.021
Incorrect Rate (μ)	0.020	0.013	0.024	0.016	0.013	0.016			
Non-Decision Time	161	161	161	161	161	161	207	207	207

Table S8

Models fitted to the Bissett and Logan (2011) data. The best-fitting model in the aggregate fits is in bold italic font.

	Go Threshold	Go Rate	Go Non-Decision Time	Stop Threshold	Stop Rate	Stop Non-Decision Time	Param	Aggregate BIC	N Fit Best
1	Fixed	Fixed	Fixed	Fixed	Fixed	Fixed	9	626377	2
2	Fixed	Fixed	Varied	Fixed	Fixed	Fixed	10	622341	2
3	Fixed	Fixed	Fixed	Varied	Varied	Varied	13	627676	0
4	Fixed	Fixed	Varied	Varied	Varied	Varied	14	623128	0
5	Varied	Fixed	Fixed	Fixed	Fixed	Fixed	11	620493	3
6	Varied	Fixed	Varied	Fixed	Fixed	Fixed	12	620204	0
7	Varied	Fixed	Varied	Varied	Varied	Varied	15	621115	2
8	Varied	Fixed	Varied	Varied	Varied	Varied	16	621378	0
9	***Fixed***	***Varied***	***Fixed***	***Fixed***	***Fixed***	***Fixed***	***11***	***620139***	***4***
10	Fixed	Varied	Varied	Fixed	Fixed	Fixed	12	620219	4
11	Fixed	Varied	Fixed	Varied	Varied	Varied	15	621101	1
12	Fixed	Varied	Varied	Varied	Varied	Varied	16	620894	0
13	Varied	Varied	Fixed	Fixed	Fixed	Fixed	13	620214	1
14	Varied	Varied	Varied	Fixed	Fixed	Fixed	14	620294	4
15	Varied	Varied	Fixed	Varied	Varied	Varied	17	621048	1
16	Varied	Varied	Varied	Varied	Varied	Varied	18	621287	0

Figure Titles

Figure S1. Mean observed (lines) and predicted (points) go response time (Go RT), signal-respond response time (SR RT), stop-signal response time (SSRT), and error rate (P(Error)) for diffusion race (Panel A) and Poisson race (Panel B) models as a function of number of choice alternatives in Experiment 1.

Figure S2. Observed (lines) and predicted (points) inhibition functions for diffusion race (Panel A) and Poisson race (Panel B) models averaged over subjects as a function of number of choice alternatives (2, 4, 6) and stop-signal delay in Experiment 1.

Figure S3. Experiment 1 diffusion race model fits. Quantile average response time distributions for no-stop-signal and signal-respond trials for the three middle stop-signal delays. The lines represent the observed data. The points represent predictions from the best diffusion race model, which assumed a limited-capacity go process and an unlimited-capacity stop process. Panel A: Two choice alternatives. Panel B: Four choice alternatives. Panel C: Six choice alternatives.

Figure S4. Experiment 1 Poisson race model fits. Quantile average response time distributions for no-stop-signal and signal-respond trials for the three middle stop-signal delays. The lines represent the observed data. The points represent predictions from the best Poisson race model, which assumed a limited-capacity go process and an unlimited-capacity stop process. Panel A: Two choice alternatives. Panel B: Four choice alternatives. Panel C: Six choice alternatives.

Figure S5. Estimated "winning" and "parent" distributions of stop-signal response time from the limited-capacity go, unlimited-capacity stop diffusion race (top) and Poisson race (bottom) models in Experiment 1.

Figure S6. Observed (lines) and predicted (points) quantile average response time distributions for correct and error responses as a function of number of choice alternatives in Experiment 1. Panel A: Diffusion race model. Panel B: Poisson race model.

Figure S7. Observed (lines) and predicted (points) quantile average response times for correct (top panel) and error (bottom panel) responses as a

function of number of choice alternatives in Experiment 1. The predicted values are from fits of the Linear Ballistic Accumulator model that assumed variable go thresholds, variable go rates, fixed stop thresholds, and fixed stop rates (model VVCC).

Figure S8. Mean observed (lines) and predicted (points) go response time (Go RT), signal-respond response time (SR RT), stop-signal response time (SSRT), and error rate (P(E)) as a function of memory set size (1, 2, 3) in Experiment 2. Target present data (Yes) are presented in the left panels. Target absent data (No) are presented in the right panels. Diffusion race model predictions are presented in the top panels. Poisson race model predictions are presented in the bottom panels.

Figure S9. Observed (lines) and predicted (points) inhibition functions for each combination of memory set size (1, 2, 3) and target presence versus absence (Yes vs. No) averaged over subjects plotted as a function of stop-signal delay in Experiment 2. Diffusion race model predictions are presented in the top panel. Poisson race model predictions are presented in the bottom panel.

Figure S10. Experiment 2 diffusion race model fits. Quantile average response time distributions for no-stop-signal and signal-respond trials for the three middle stop-signal delays. The lines represent the observed data. The points represent predictions from the best diffusion race model, which assumed a limited-capacity go process and an unlimited-capacity stop process. Panel A: Memory set size 1. Panel B: Memory set size 2. Panel C: Memory set size 3.

Figure S11. Experiment 2 Poisson race model fits. Quantile average response time distributions for no-stop-signal and signal-respond trials for the three middle stop-signal delays. The lines represent the observed data. The points represent predictions from the best Poisson race model, which assumed a limited-capacity go process and an unlimited-capacity stop process. Panel A: Memory set size 1. Panel B: Memory set size 2. Panel C: Memory set size 3.

Figure S12. Estimated “winning” and “parent” distributions of stop-signal response time from the limited-capacity go, unlimited-capacity stop diffusion race (top) and Poisson race (bottom) models in Experiment 2.

Figure S13. Observed (lines) and predicted (points) quantile average response time distributions for correct and error target-present (left) and target-absent (right) responses as a function of memory set size in Experiment 2. Top panel: Diffusion race model. Bottom panel: Poisson race model.

Figure S14. Observed and predicted go response times from no-stop-signal and signal-respond trials, stop-signal response times, and error rates from Bissett and Logan (2011) as a function of stop-signal percentage.

Figure S15. Observed and predicted signal-respond and no-stop-signal response time distributions as a function of stop-signal percentage from the Bissett and Logan (2011) data.

Figure S16. Best-fitting parameter values for the fits to the Bissett and Logan (2011) data as a function of stop signal percentage.

Figure S17. Predicted distributions of stop-signal response times for the 20% and 40% stop signal conditions in Bissett and Logan (2011).

Figure S18. Observed and predicted distributions of correct and error response times for no-stop-signal trials as a function of stop-signal percentage in Bissett and Logan (2011). Top panels: cumulative distribution functions; Bottom panels: defective distributions.

Figure S1

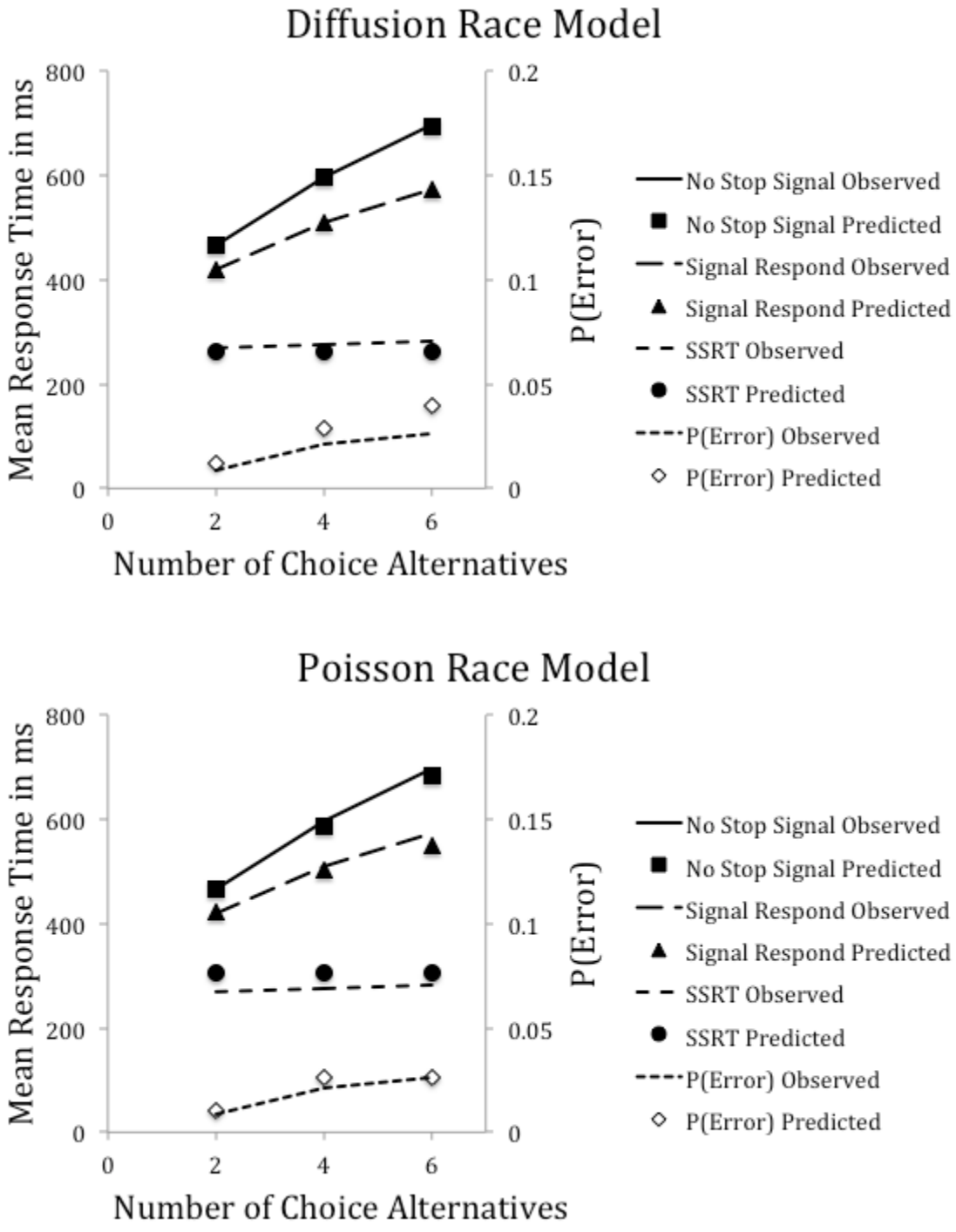
Diffusion Race Model
Mean Response Time in ms
P(Error)
Number of Choice Alternatives
800
600
400
200
0
0.2
0.15
0.1
0.05
0
0
2
4
6
No Stop Signal Observed
No Stop Signal Predicted
Signal Respond Observed
Signal Respond Predicted
SSRT Observed
SSRT Predicted
P(Error) Observed
P(Error) Predicted
Poisson Race Model
Mean Response Time in ms
P(Error)
Number of Choice Alternatives
800
600
400
200
0
0.2
0.15
0.1
0.05
0
0
2
4
6
No Stop Signal Observed
No Stop Signal Predicted
Signal Respond Observed
Signal Respond Predicted
SSRT Observed
SSRT Predicted
P(Error) Observed
P(Error) Predicted

Figure S2

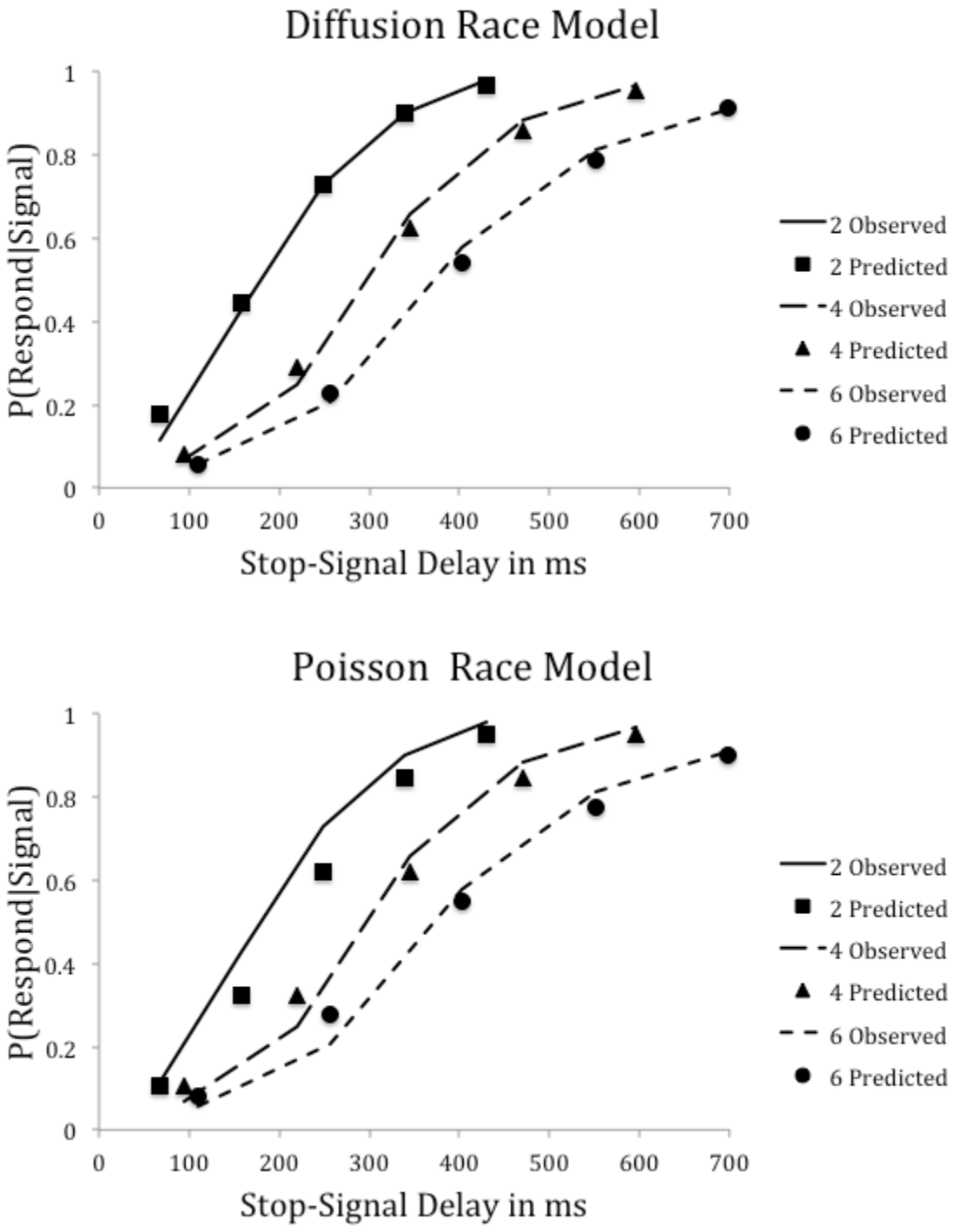
Diffusion Race Model
P(Respond|Signal)
1
0.8
0.6
0.4
0.2
0
0
100
200
300
400
500
600
700
Stop-Signal Delay in ms
2 Observed
2 Predicted
4 Observed
4 Predicted
6 Observed
6 Predicted
Poisson Race Model
P(Respond|Signal)
1
0.8
0.6
0.4
0.2
0
0
100
200
300
400
500
600
700
Stop-Signal Delay in ms
2 Observed
2 Predicted
4 Observed
4 Predicted
6 Observed
6 Predicted

Figure S3

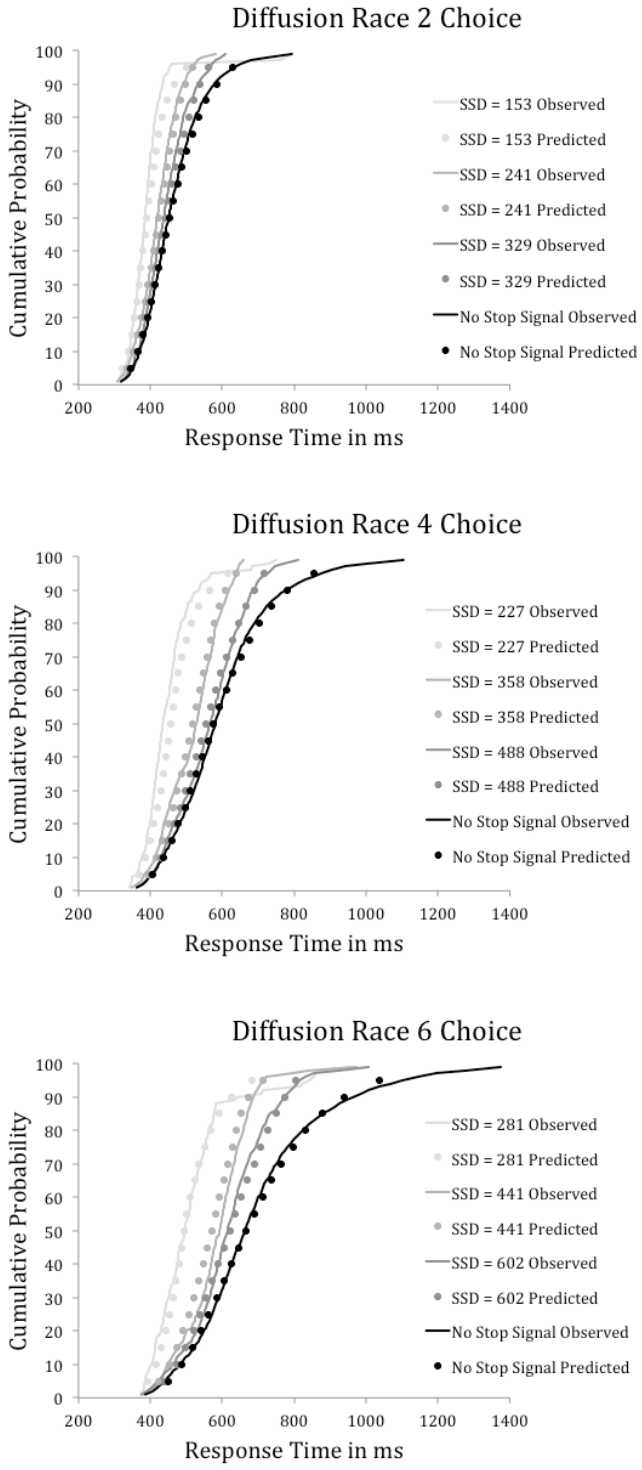
Diffusion Race 2 Choice
Cumulative Probability
Response Time in ms
SSD = 153 Observed
SSD = 153 Predicted
SSD = 241 Observed
SSD = 241 Predicted
SSD = 329 Observed
SSD = 329 Predicted
No Stop Signal Observed
No Stop Signal Predicted
Diffusion Race 4 Choice
Cumulative Probability
Response Time in ms
SSD = 227 Observed
SSD = 227 Predicted
SSD = 358 Observed
SSD = 358 Predicted
SSD = 488 Observed
SSD = 488 Predicted
No Stop Signal Observed
No Stop Signal Predicted
Diffusion Race 6 Choice
Cumulative Probability
Response Time in ms
SSD = 281 Observed
SSD = 281 Predicted
SSD = 441 Observed
SSD = 441 Predicted
SSD = 602 Observed
SSD = 602 Predicted
No Stop Signal Observed
No Stop Signal Predicted

Figure S4

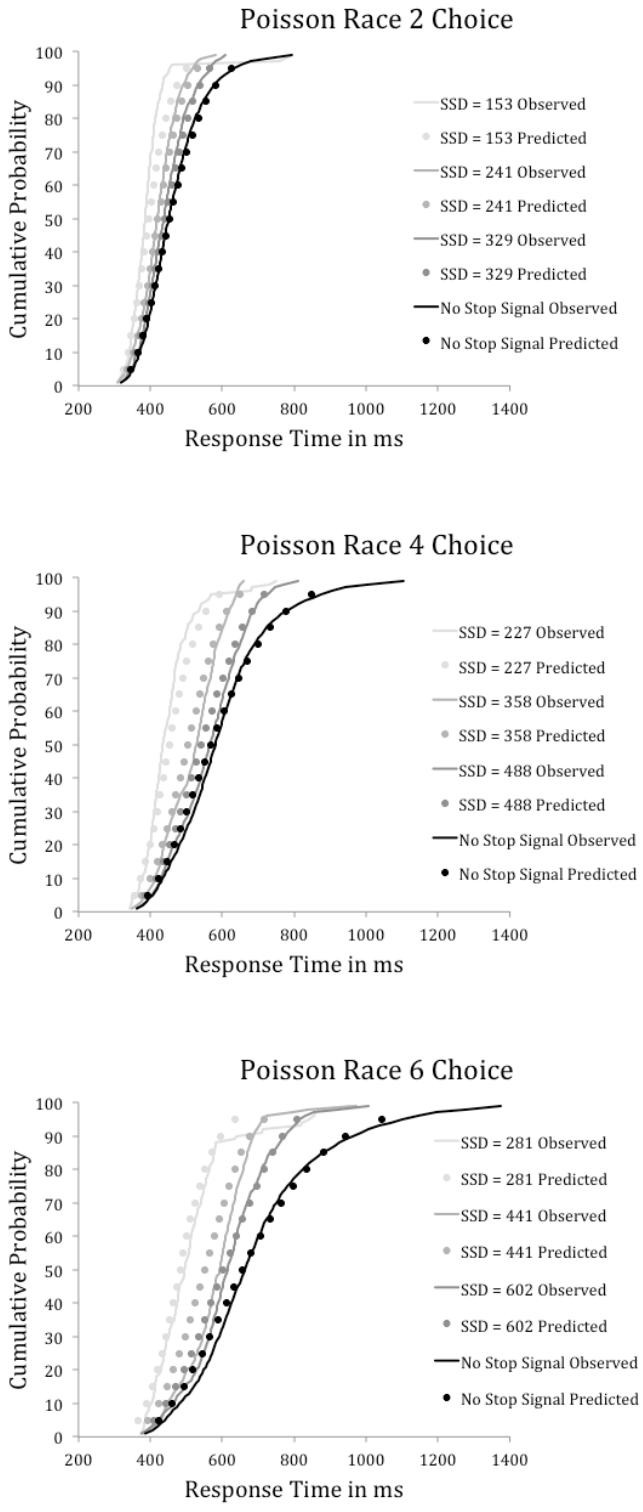
Poisson Race 2 Choice
Cumulative Probability
Response Time in ms
SSD = 153 Observed
SSD = 153 Predicted
SSD = 241 Observed
SSD = 241 Predicted
SSD = 329 Observed
SSD = 329 Predicted
No Stop Signal Observed
No Stop Signal Predicted
Poisson Race 4 Choice
Cumulative Probability
Response Time in ms
SSD = 227 Observed
SSD = 227 Predicted
SSD = 358 Observed
SSD = 358 Predicted
SSD = 488 Observed
SSD = 488 Predicted
No Stop Signal Observed
No Stop Signal Predicted
Poisson Race 6 Choice
Cumulative Probability
Response Time in ms
SSD = 281 Observed
SSD = 281 Predicted
SSD = 441 Observed
SSD = 441 Predicted
SSD = 602 Observed
SSD = 602 Predicted
No Stop Signal Observed
No Stop Signal Predicted

Figure S5

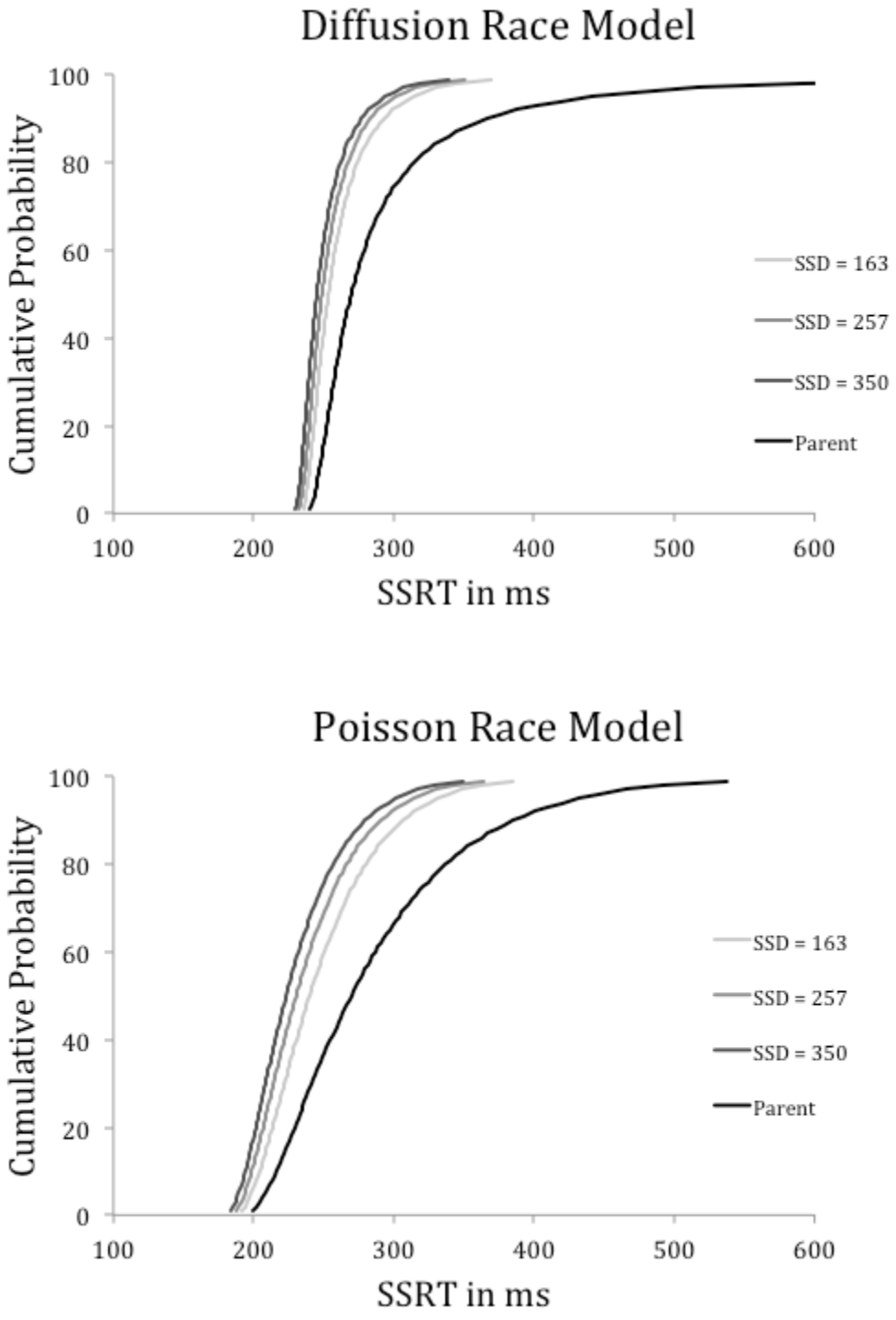
Diffusion Race Model
Cumulative Probability
100
80
60
40
20
0
100
200
300
400
500
600
SSRT in ms
SSD = 163
SSD = 257
SSD = 350
Parent
Poisson Race Model
Cumulative Probability
100
80
60
40
20
0
100
200
300
400
500
600
SSRT in ms
SSD = 163
SSD = 257
SSD = 350
Parent

Figure S6

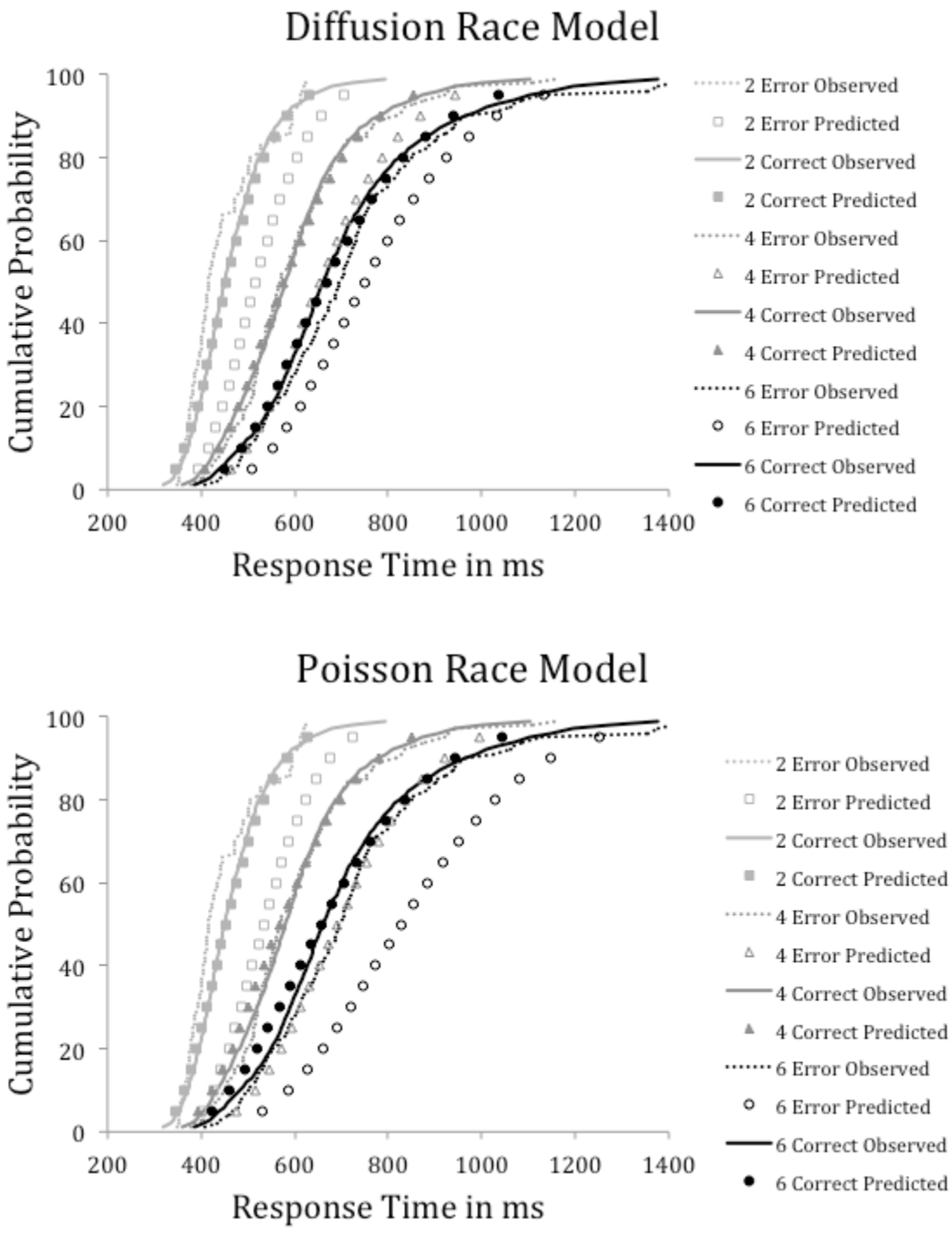
Diffusion Race Model
Cumulative Probability
Response Time in ms
2 Error Observed
2 Error Predicted
2 Correct Observed
2 Correct Predicted
4 Error Observed
4 Error Predicted
4 Correct Observed
4 Correct Predicted
6 Error Observed
6 Error Predicted
6 Correct Observed
6 Correct Predicted
Poisson Race Model
Cumulative Probability
Response Time in ms
2 Error Observed
2 Error Predicted
2 Correct Observed
2 Correct Predicted
4 Error Observed
4 Error Predicted
4 Correct Observed
4 Correct Predicted
6 Error Observed
6 Error Predicted
6 Correct Observed
6 Correct Predicted

Figure S7

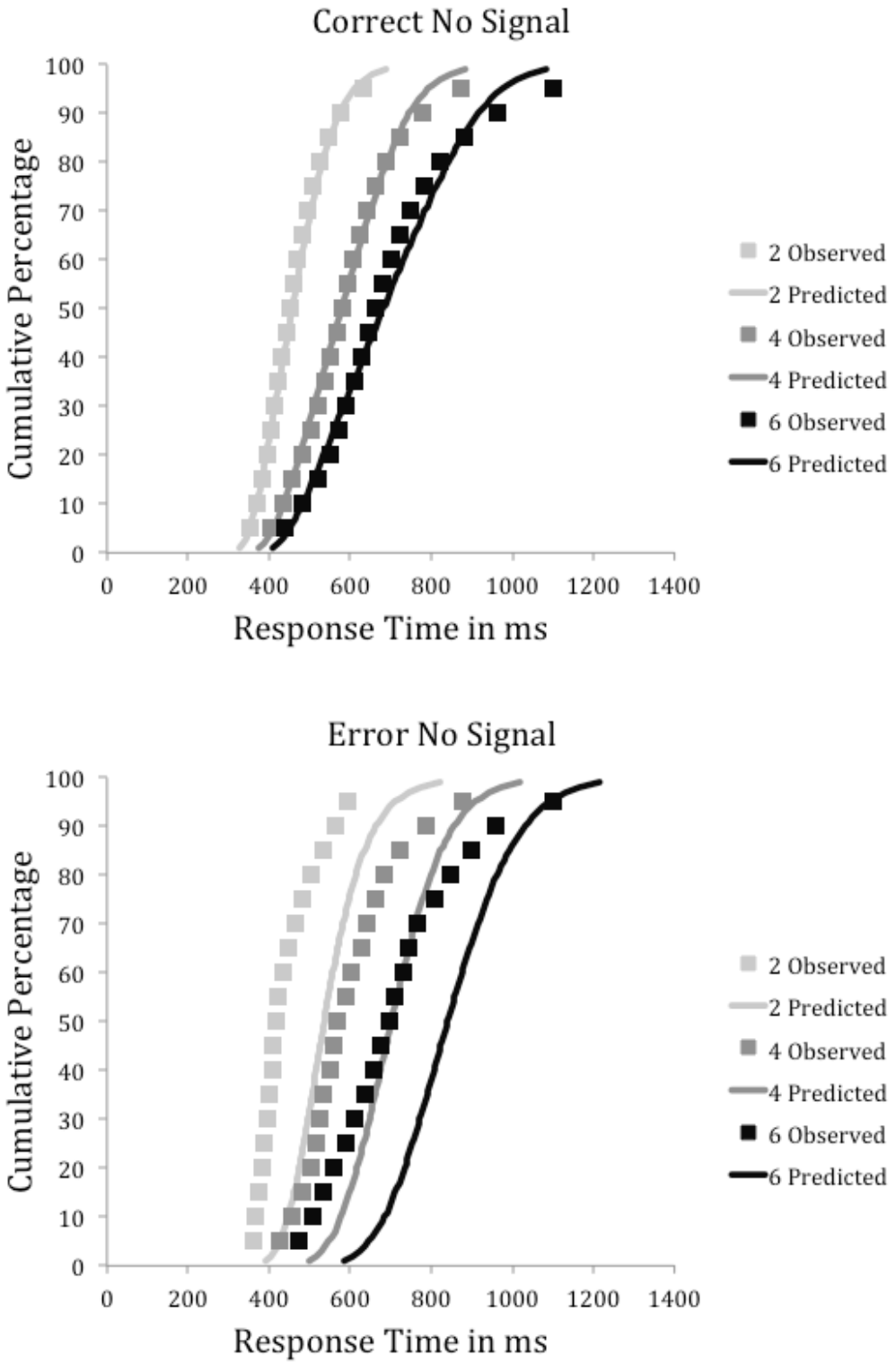
Correct No Signal
Cumulative Percentage
Response Time in ms
0
10
20
30
40
50
60
70
80
90
100
0
200
400
600
800
1000
1200
1400
2 Observed
2 Predicted
4 Observed
4 Predicted
6 Observed
6 Predicted
Error No Signal
Cumulative Percentage
Response Time in ms
2 Observed
2 Predicted
4 Observed
4 Predicted
6 Observed
6 Predicted

Figure S8, left panel

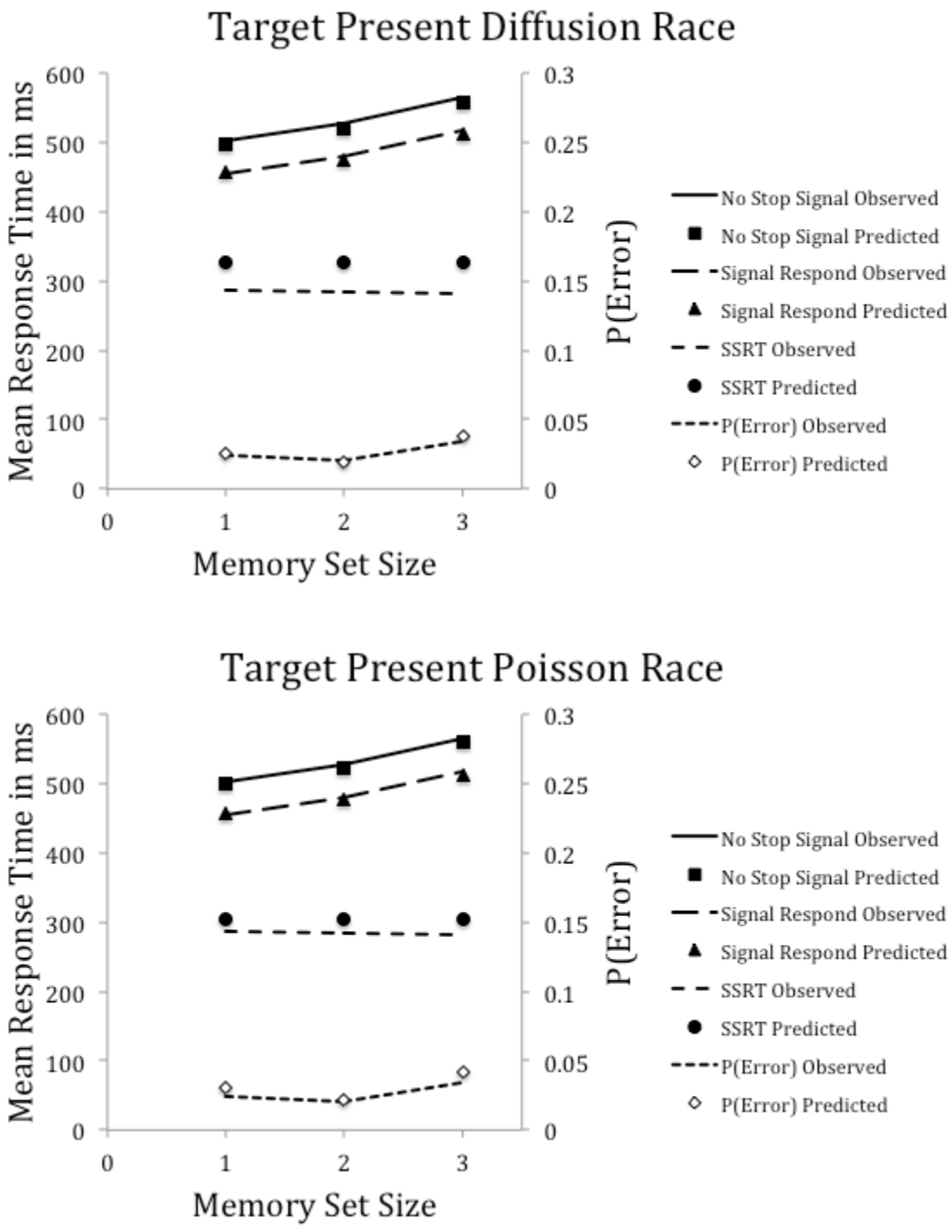

Figure S8, right panel

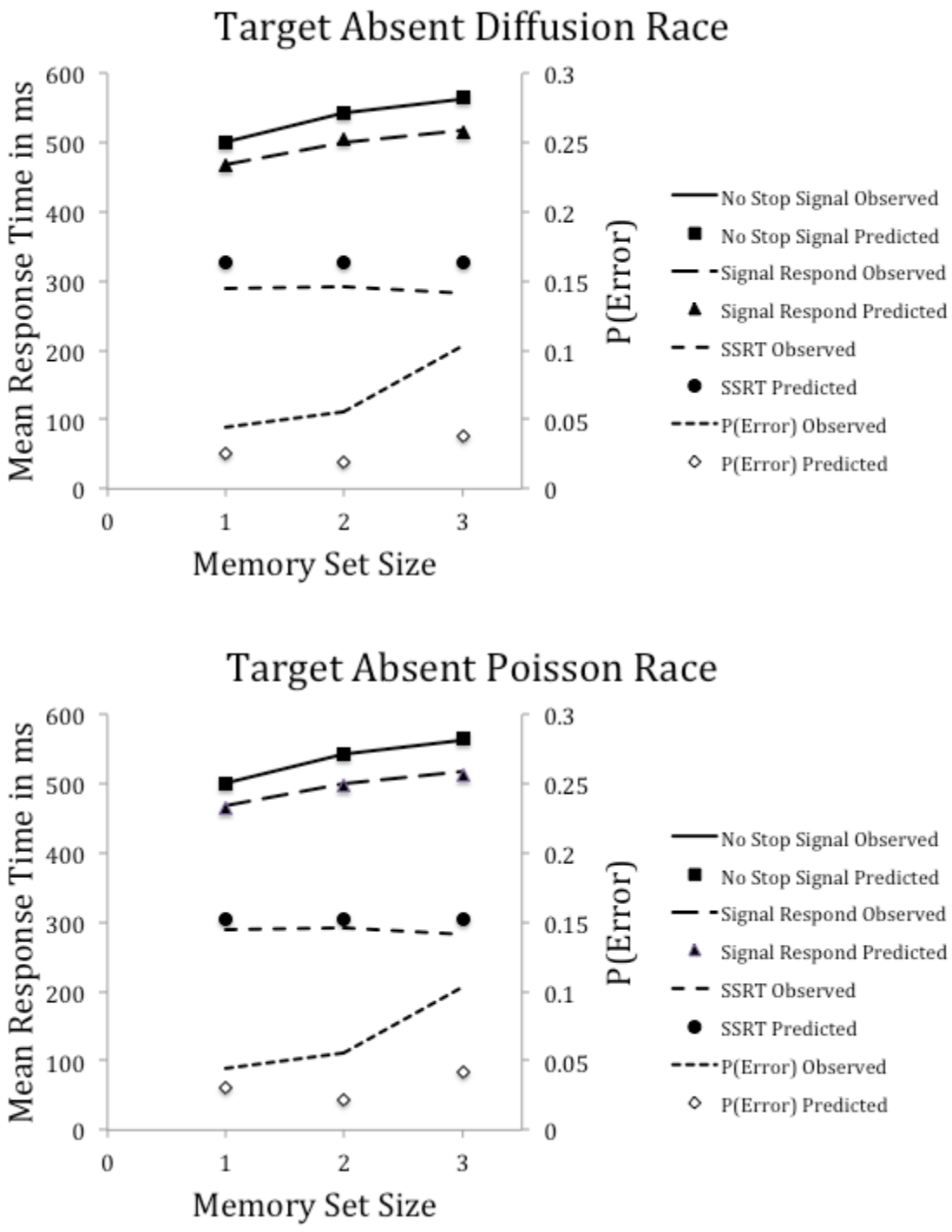

Figure S9, left panel

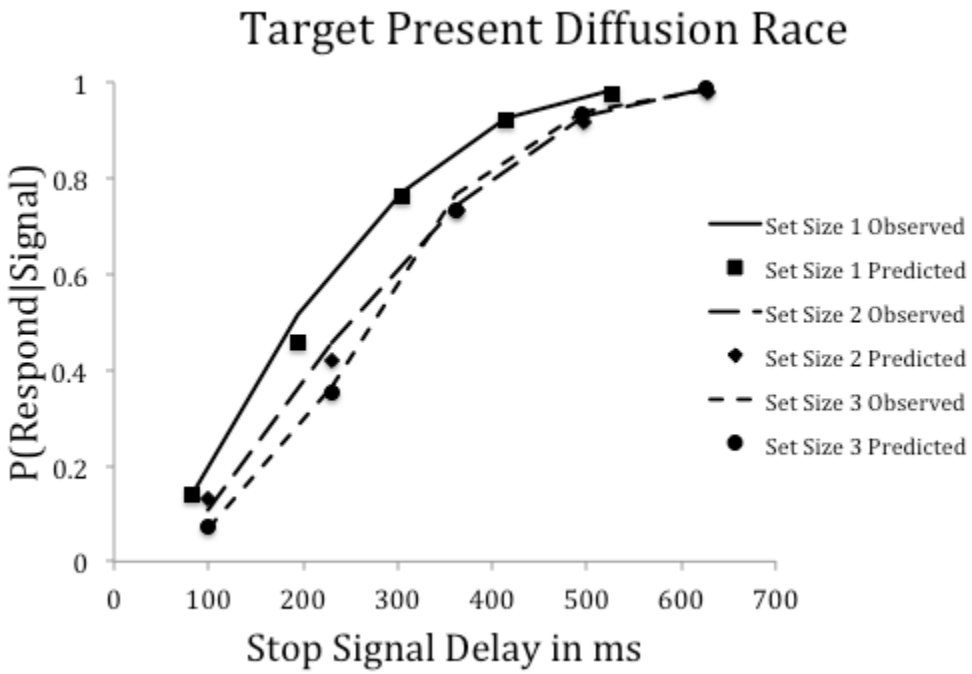

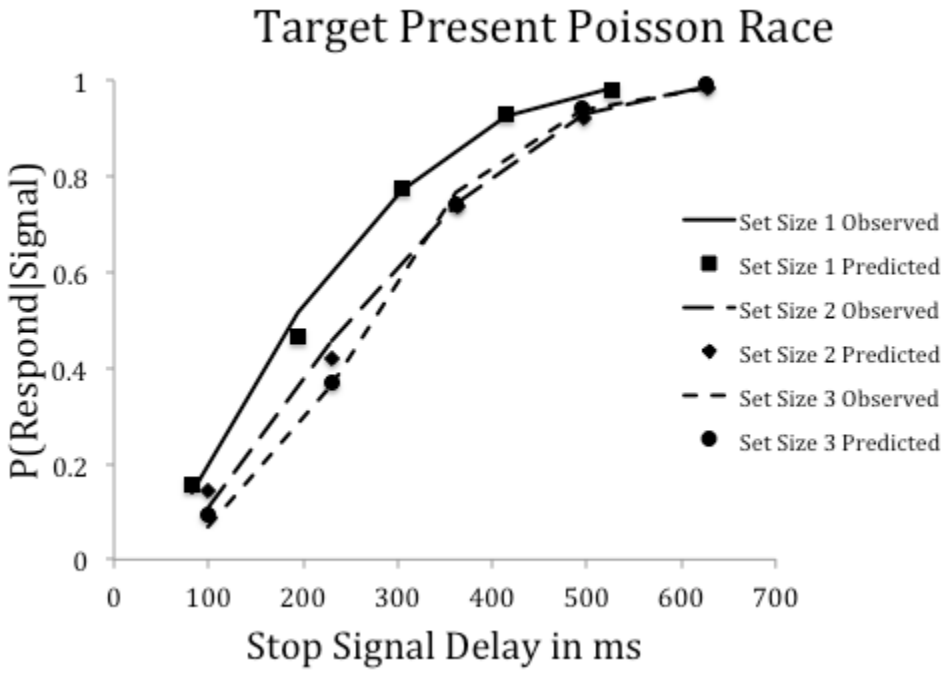

Figure S9, right panel

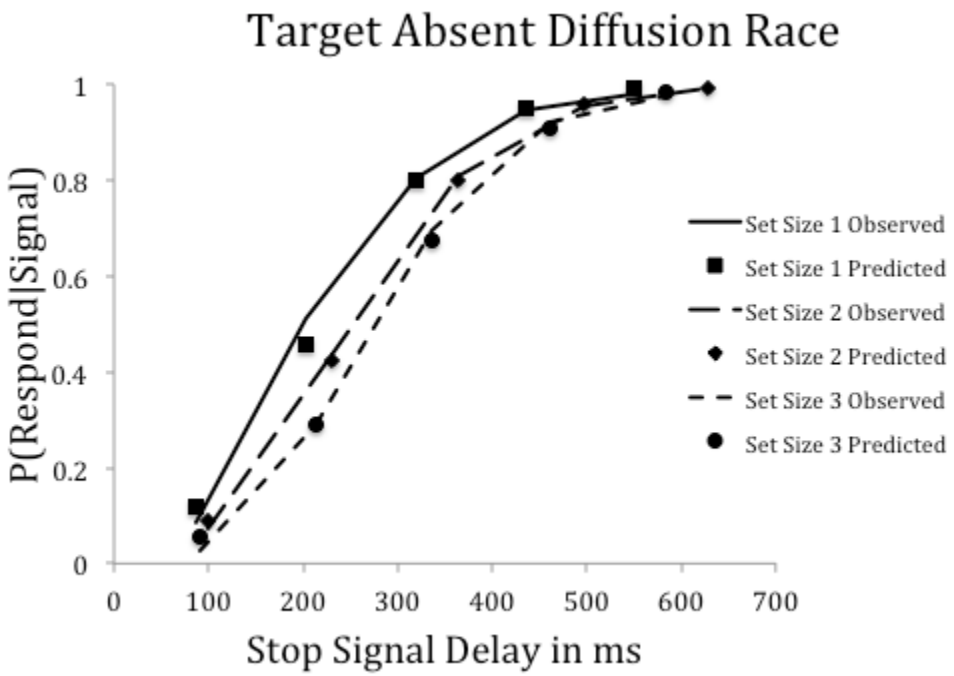

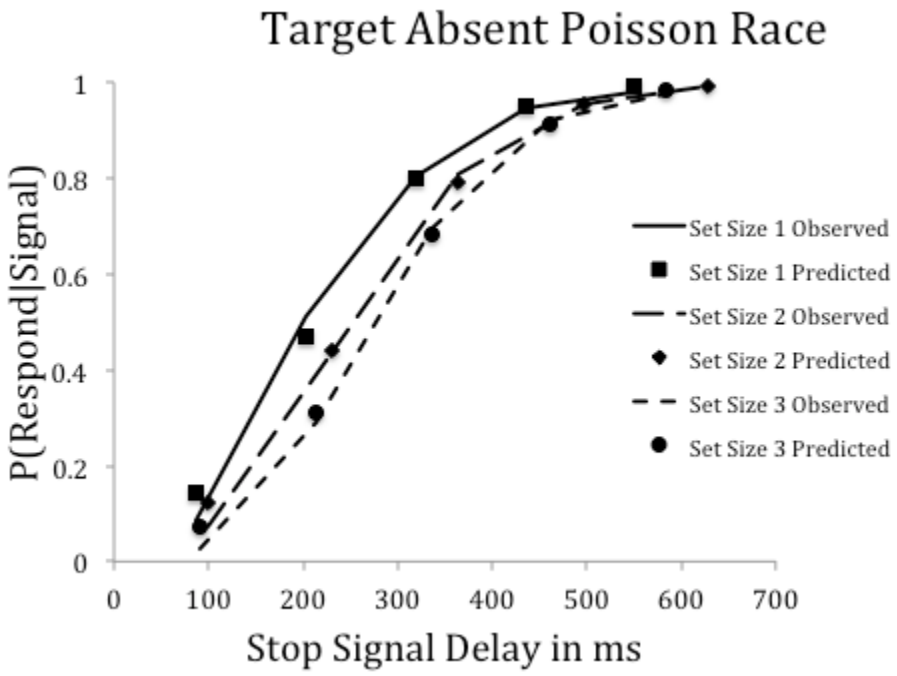

Figure S10, left panel

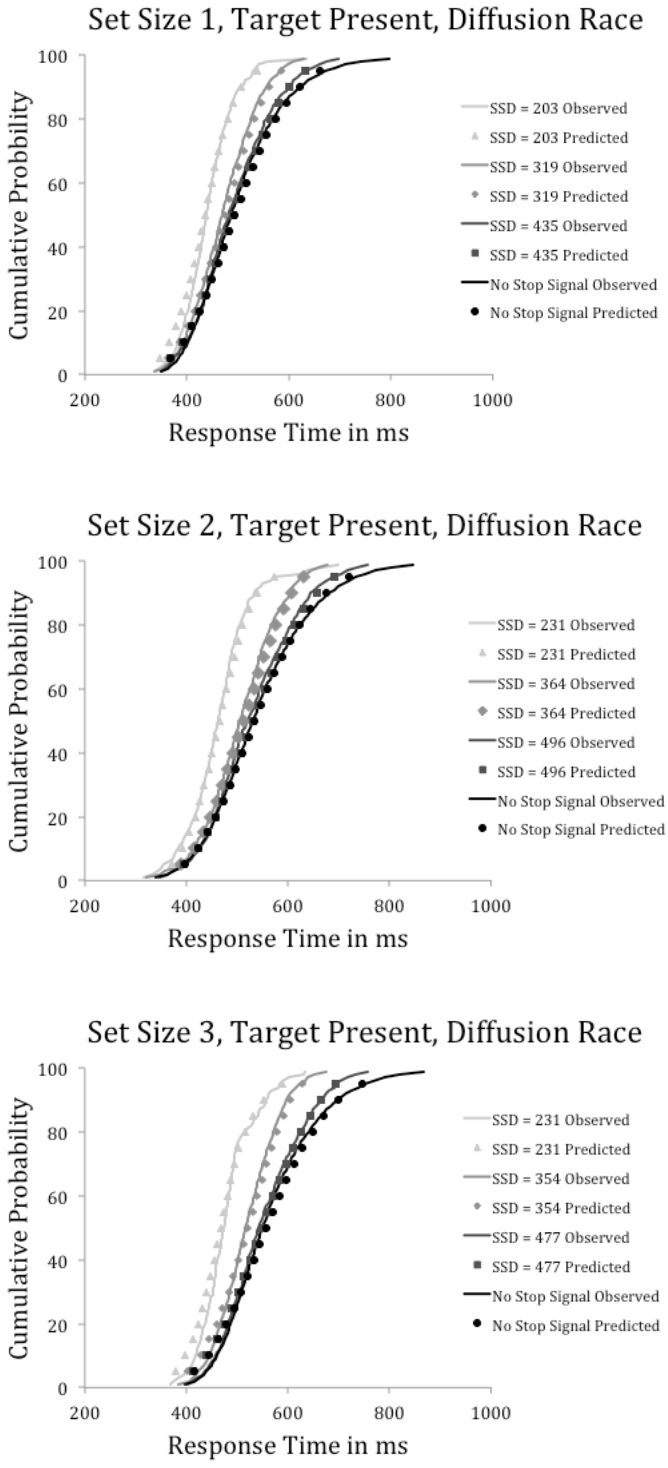

Figure S10, right panel

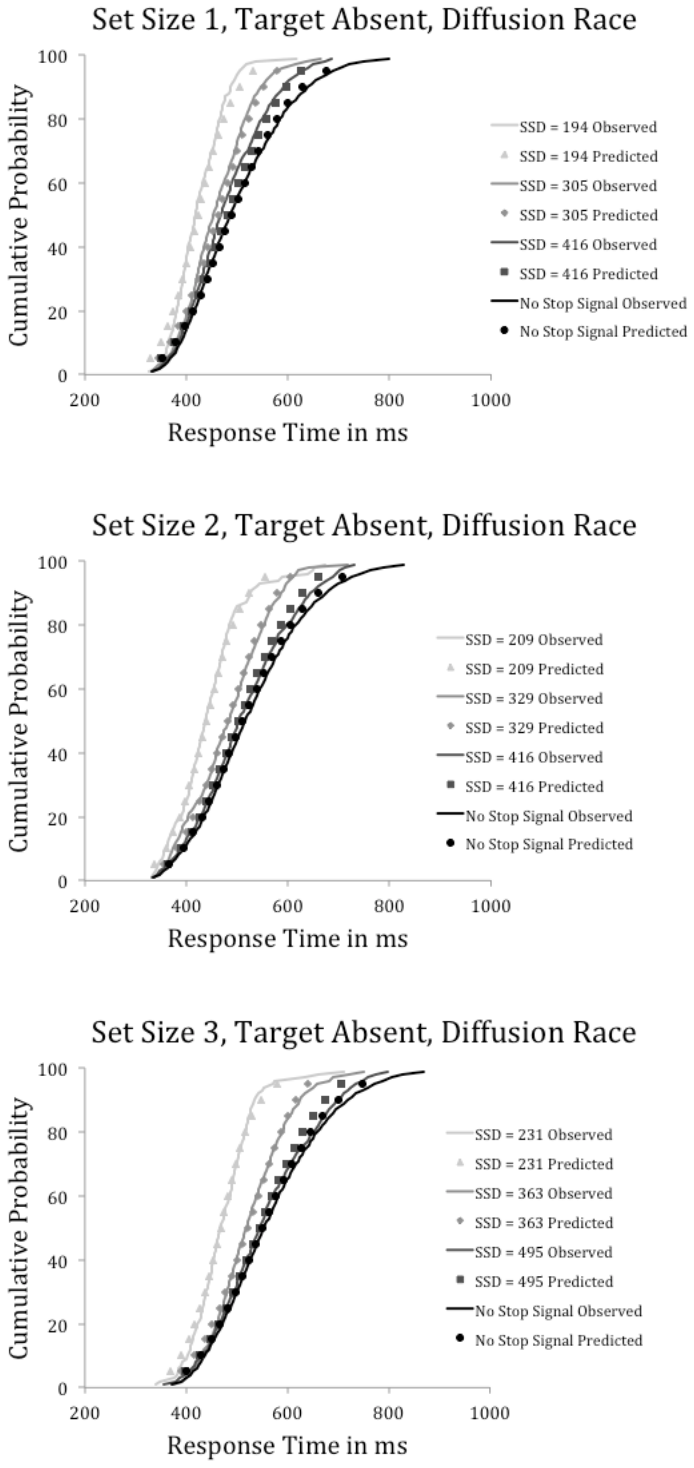

Figure S11, left panel

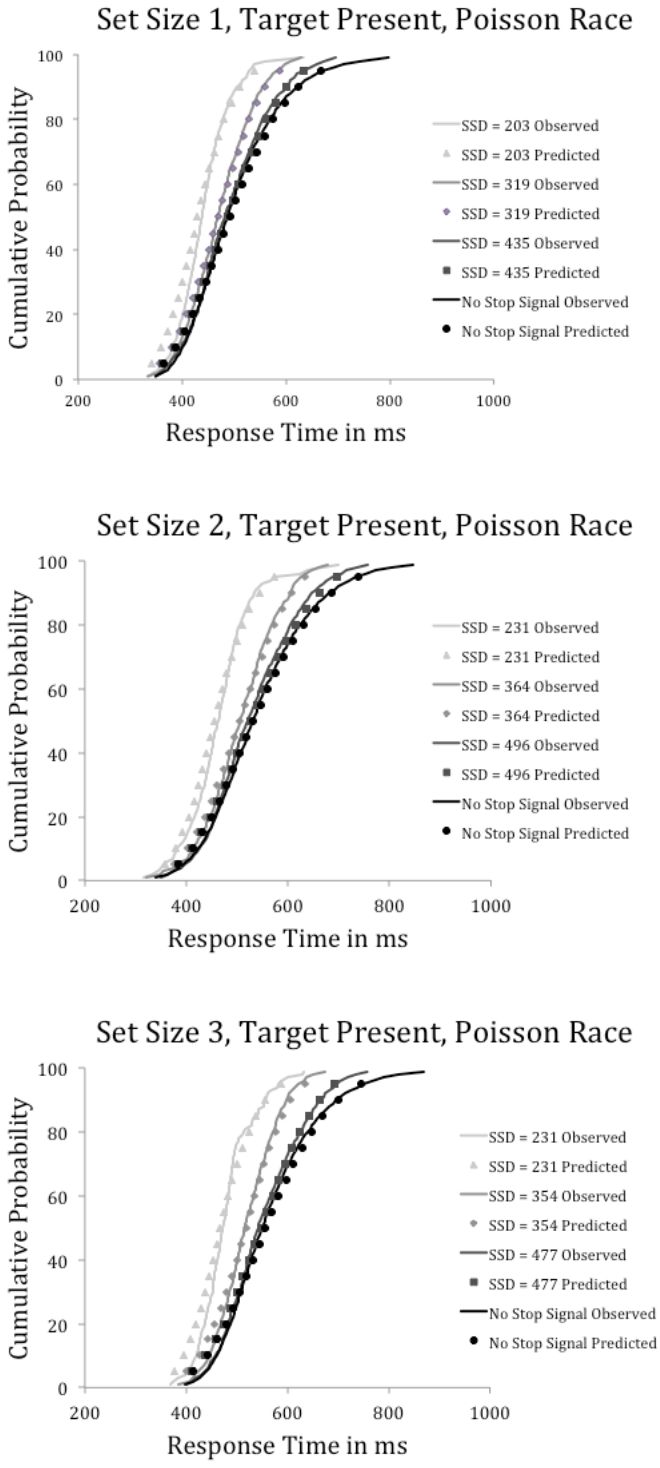

Figure S11, right panel

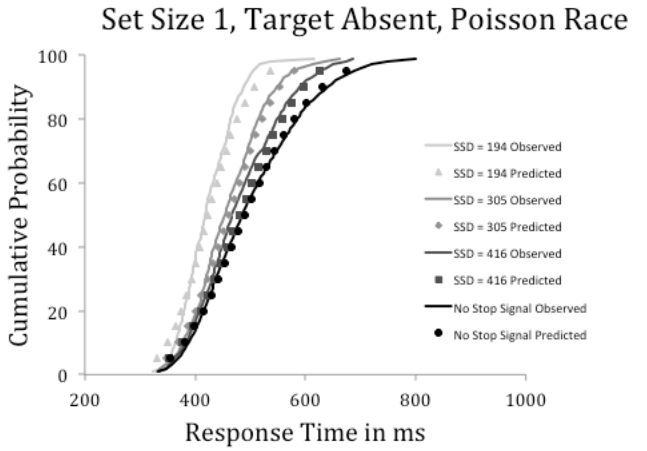

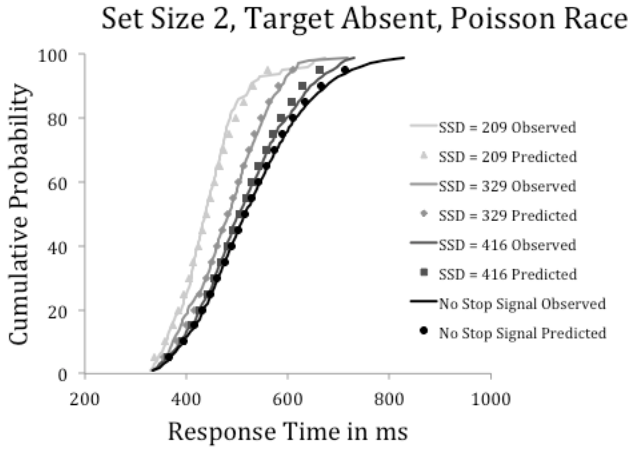

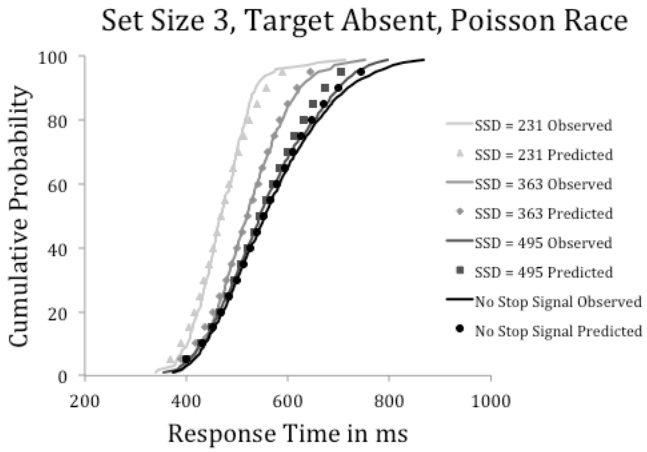

Figure S12

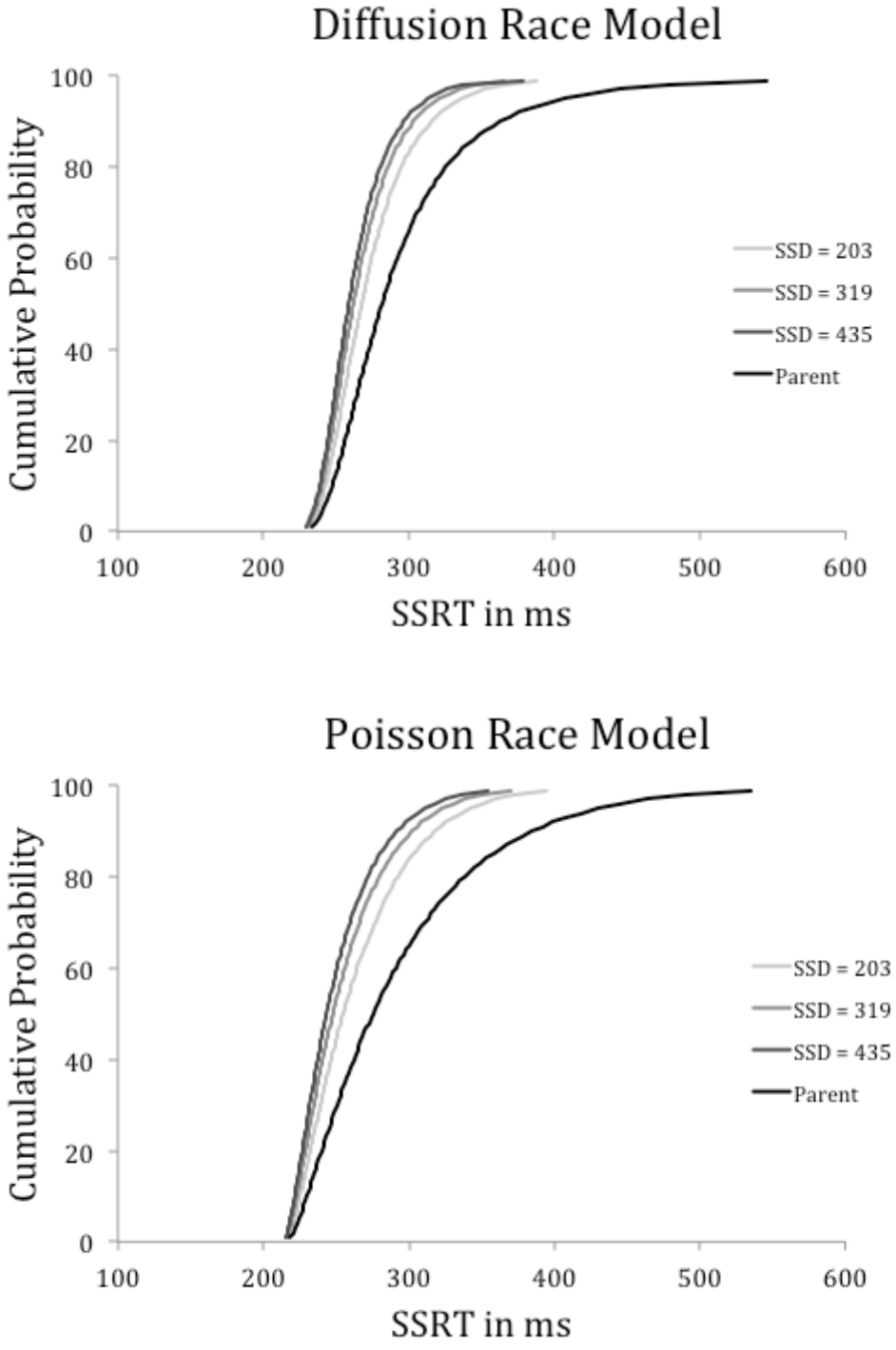
Diffusion Race Model
Cumulative Probability
100
80
60
40
20
0
100
200
300
400
500
600
SSRT in ms
SSD = 203
SSD = 319
SSD = 435
Parent
Poisson Race Model
Cumulative Probability
100
80
60
40
20
0
100
200
300
400
500
600
SSRT in ms
SSD = 203
SSD = 319
SSD = 435
Parent

Figure S13, left panel

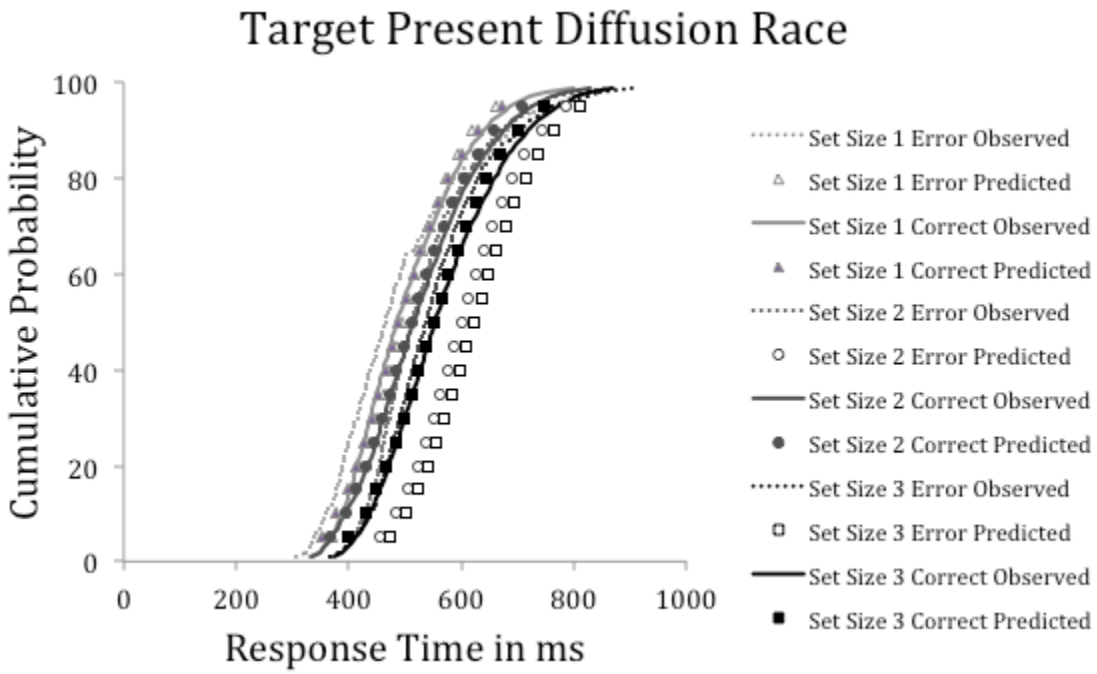

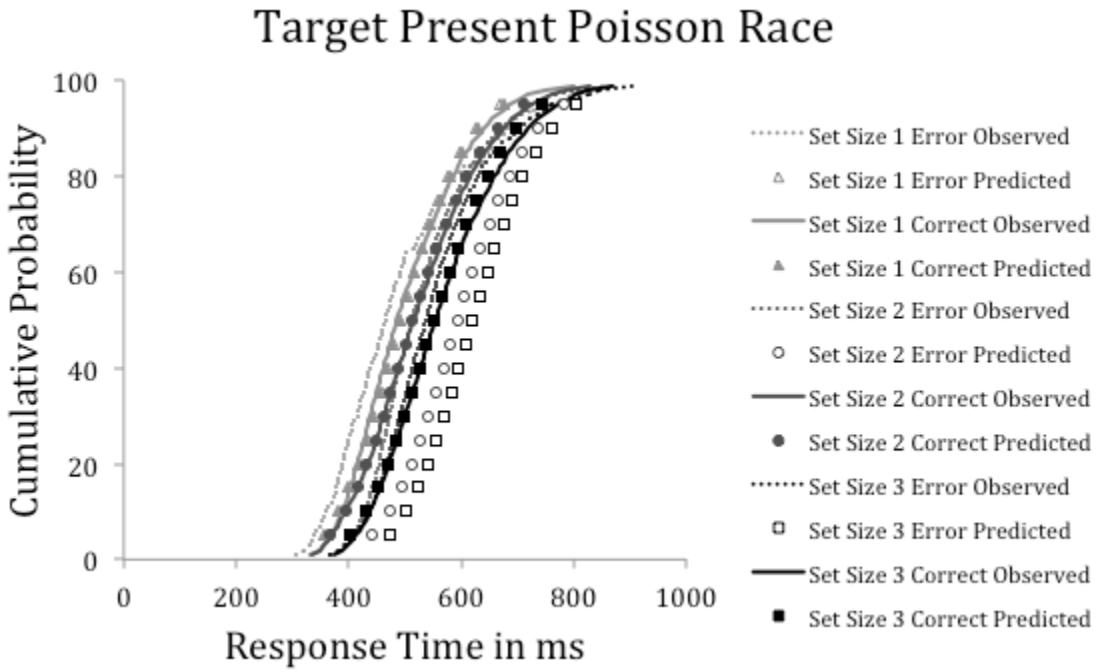

Figure S13, right panel

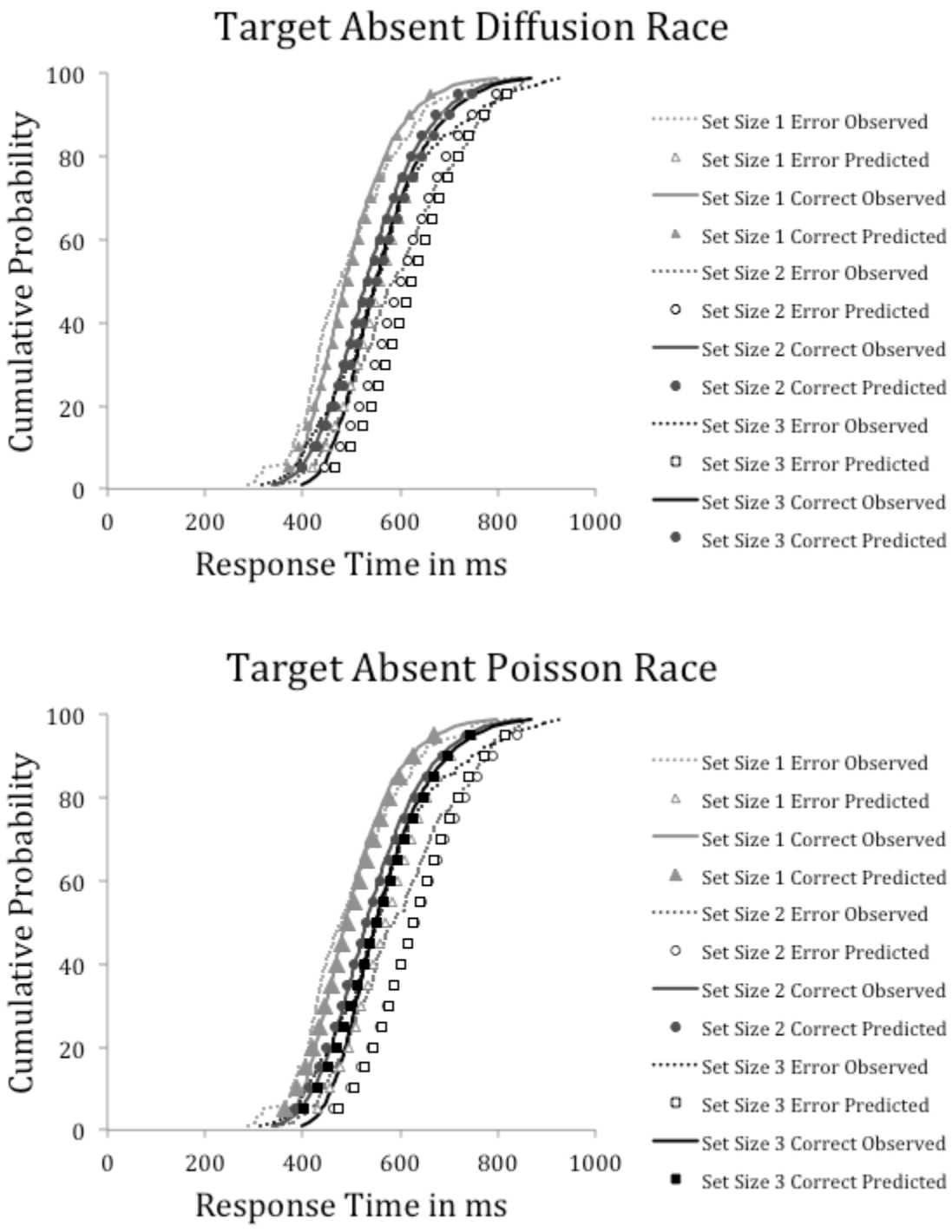

Figure S14

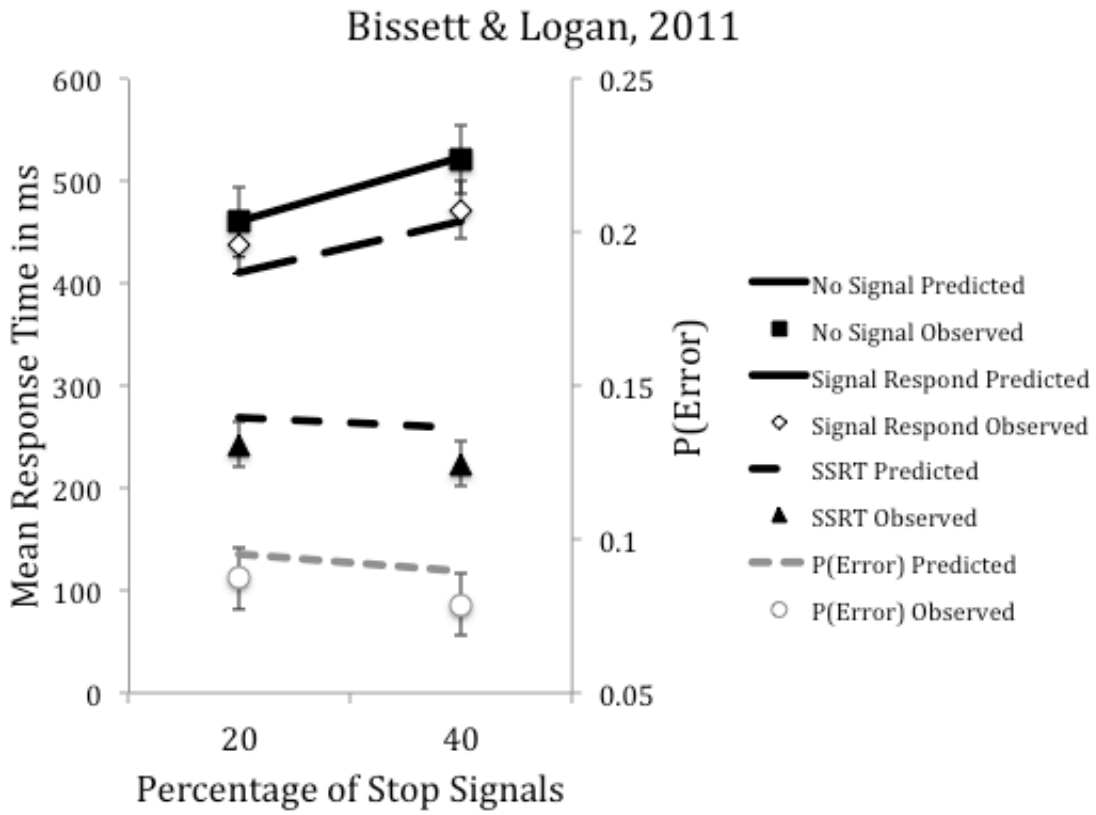
Bissett & Logan, 2011
Mean Response Time in ms
600
500
400
300
200
100
0
0.25
0.2
0.15
0.1
0.05
P(Error)
20
40
Percentage of Stop Signals
No Signal Predicted
No Signal Observed
Signal Respond Predicted
Signal Respond Observed
SSRT Predicted
SSRT Observed
P(Error) Predicted
P(Error) Observed

Figure S15

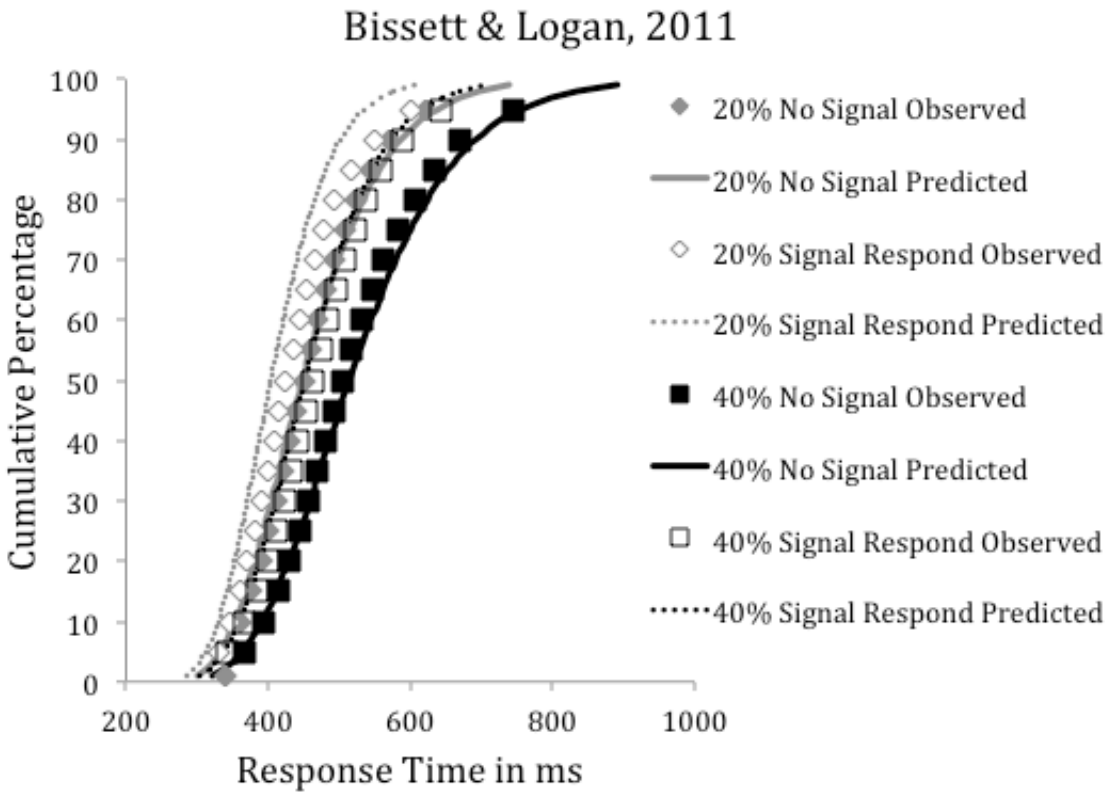
Bissett & Logan, 2011
Cumulative Percentage
100
90
80
70
60
50
40
30
20
10
0
200
400
600
800
1000
Response Time in ms
20% No Signal Observed
20% No Signal Predicted
20% Signal Respond Observed
20% Signal Respond Predicted
40% No Signal Observed
40% No Signal Predicted
40% Signal Respond Observed
40% Signal Respond Predicted

Figure S16

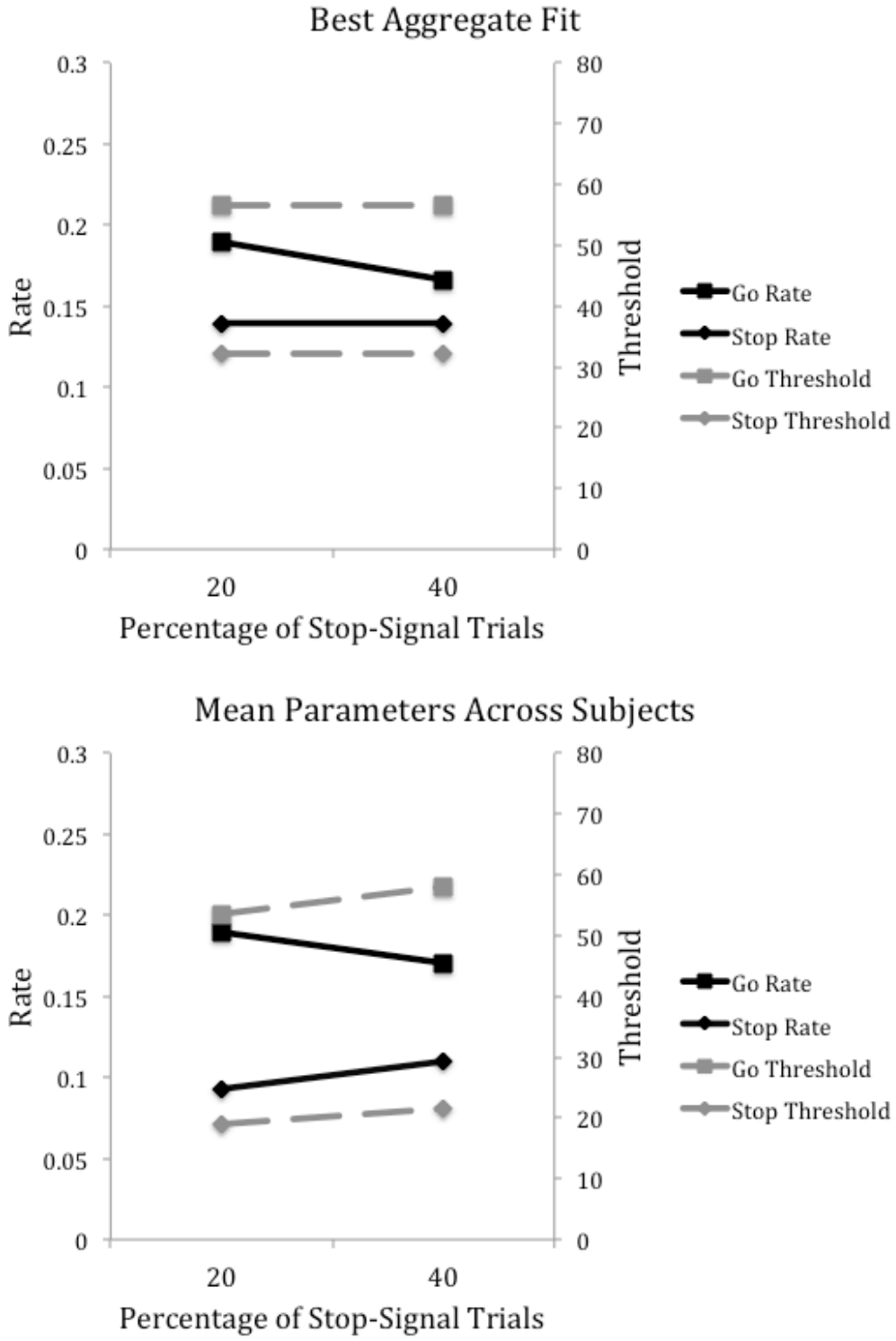
Best Aggregate Fit
Rate
Threshold
0.3
0.25
0.2
0.15
0.1
0.05
0
80
70
60
50
40
30
20
10
0
20
40
Percentage of Stop-Signal Trials
Go Rate
Stop Rate
Go Threshold
Stop Threshold
Mean Parameters Across Subjects
Rate
Threshold
0.3
0.25
0.2
0.15
0.1
0.05
0
80
70
60
50
40
30
20
10
0
20
40
Percentage of Stop-Signal Trials
Go Rate
Stop Rate
Go Threshold
Stop Threshold

Figure S17

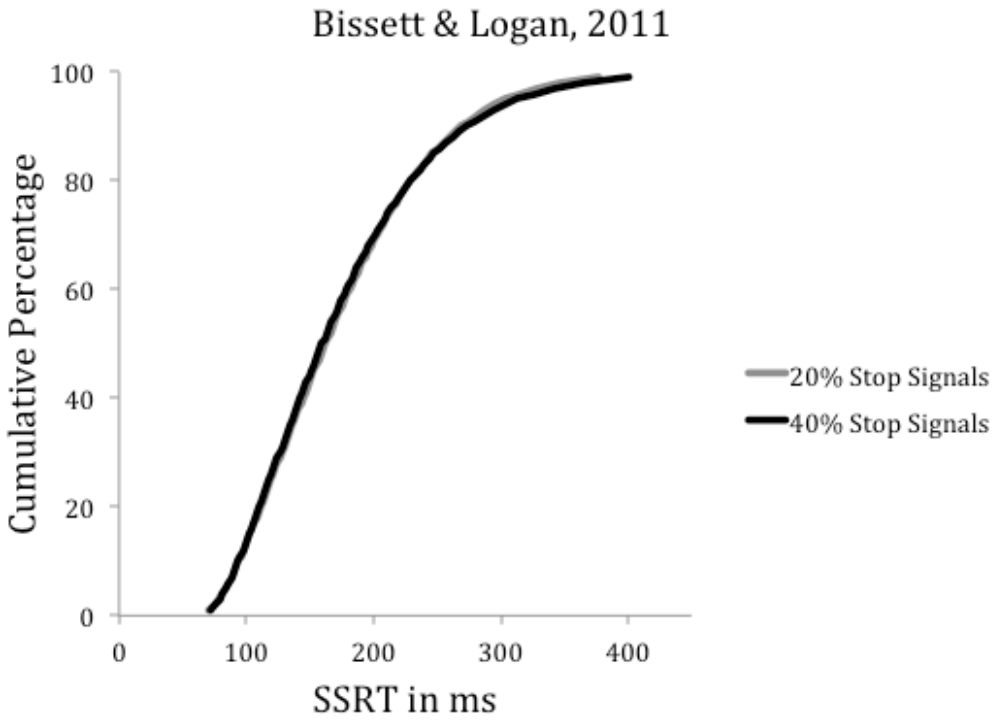
Bissett & Logan, 2011
Cumulative Percentage
100
80
60
40
20
0
0
100
200
300
400
SSRT in ms
20% Stop Signals
40% Stop Signals

Figure S18

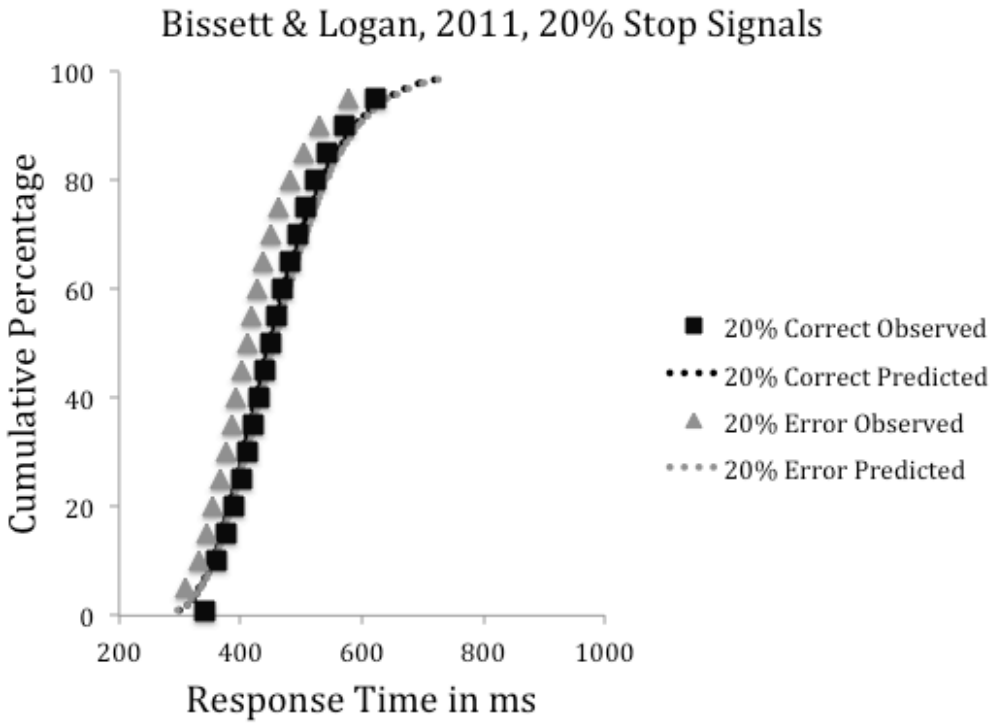
Bissett & Logan, 2011, 20% Stop Signals
Cumulative Percentage
100
80
60
40
20
0
200
400
600
800
1000
Response Time in ms
20% Correct Observed
20% Correct Predicted
20% Error Observed
20% Error Predicted

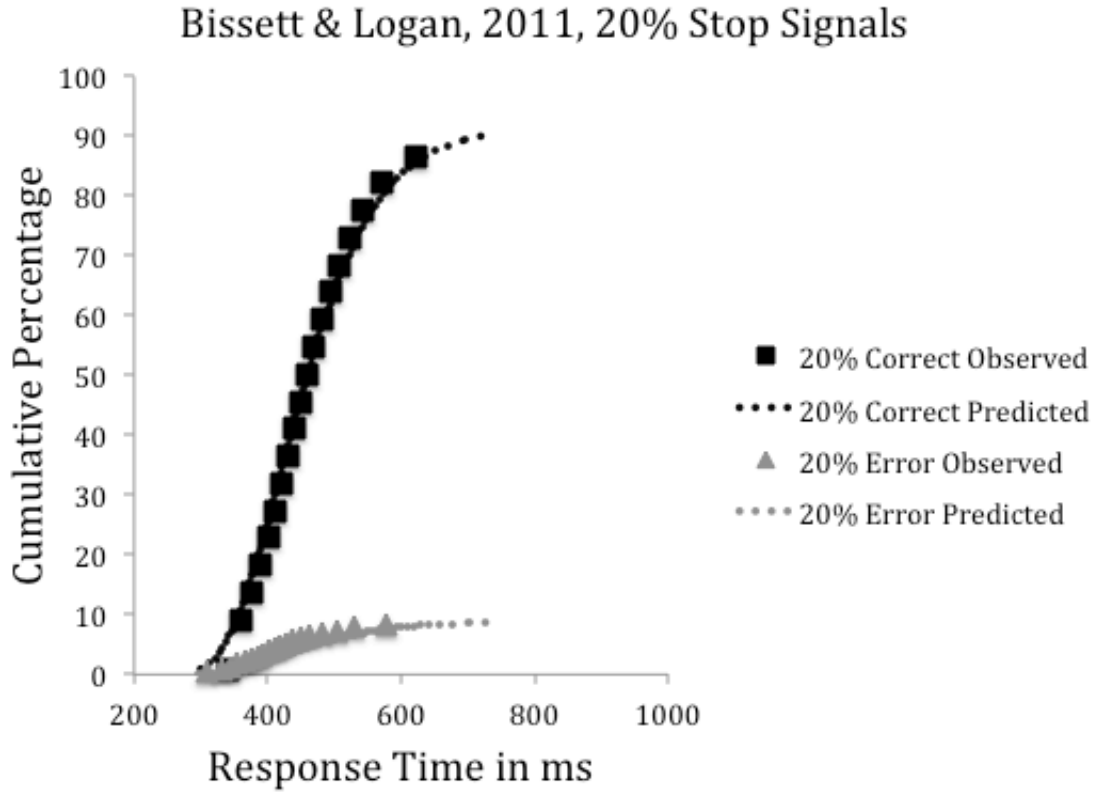
Bissett & Logan, 2011, 20% Stop Signals
Cumulative Percentage
100
90
80
70
60
50
40
30
20
10
0
200
400
600
800
1000
Response Time in ms
20% Correct Observed
20% Correct Predicted
20% Error Observed
20% Error Predicted

Figure S18 continued